ICARUS 118, 132–154 (1995)

Asteroid Families Close to Mean Motion Resonances: Dynamical Effects and Physical Implications

A. MORBIDELLI

OCA, Observatoire de Nice, BP 229, F-06304 Nice Cedex 4, France

V. ZAPPALÀ

Osservatorio Astronomico di Torino, I-10025 Pino Torinese (TO), Italy

M. MOONS

Département de Mathématiques, FUNDP, 8 Rempart de la Vierge, B-5000, Namur, Belgium
E-mail: mmoons@cc.fundp.ac.be

A. CELLINO

Osservatorio Astronomico di Torino, I-10025 Pino Torinese (TO), Italy

AND

R. GONCZI

OCA, Observatoire de Nice, BP 229, F-06304 Nice Cedex 4, France

Received December 19, 1994; revised June 14, 1995

Among the asteroid families which can be considered very reliable according to the results of the most recent and objective methods of statistical identification, some are located very close to mean motion resonances with Jupiter. A careful analysis of the dynamical behavior of the candidate members in proximity of the resonances, combined with the known kinematical properties of the families at different size ranges, strongly suggests that the global structure of some families could have been significantly affected by the resonance proximity. This is true even in the cases of mean motion resonances, which are not among the most efficient and fastest commonly known depleters of asteroidal orbits. The most outstanding results of this paper concern the Eos and the Themis family, affected, respectively, by the 9/4 and 2/1 resonances. Both families seem to have been significantly depleted by these two resonances. Among the families showing a quasi-isotropic structure, Gefion and Dora appear to have injected a substantial fraction of their original members into the 5/2 mean motion resonance, while Adeona seems to have been only marginally affected by the 8/3. On the other hand, the irregular and/or complex structures of the Eunomia, Nysa, and Maria families prevent us from drawing any definitive conclusion. Finally, for the family of Hygiea, a quite strong depleting role of the 2/1 resonance is also suggested.

1. INTRODUCTION

Important improvements of the statistical techniques of asteroid family identification have been achieved in the last few years (Zappalà *et al.* 1990; Bendjoya *et al.* 1991; Lindblad 1992; Bendjoya 1993; Bendjoya *et al.* 1993; Lindblad 1994; Zappalà *et al.* 1994, 1995; Zappalà and Cellino 1994). These developments have been triggered by the simultaneous improvements of the techniques of computation of asteroid proper elements (Milani and Knežević 1990, 1992, 1994; Knežević and Milani 1994).

As a result, we have now at our disposal a list of candidate families whose reliability is stated on the basis of a solid statistical background. Several of these families are found very close to some mean motion resonance with Jupiter, and the aim of this paper is to understand if and how resonances may have affected their structure. The relevance of this question from the physical viewpoint is evident. First, if one can prove that a family has injected a significative fraction of its members into a resonance associated with a Kirkwood gap, it is plausible to assume that the parent body breakup has been a relevant source of near Earth asteroids (NEAs) and meteorites, possibly of large size. Second, in order to derive from family structures

0019-1035/95 $12.00

information on the large-scale collisions responsible for their origin, it is important to assess whether the observed asymmetries are due to dynamical reasons rather than to the characteristics of the breakup events.

Let us detail further this second point. Families are believed to have originated by the (collisional) catastrophic disruption of single parent bodies, and direct observations of different members of the same family have allowed in some cases a confirmation of the hypothesis of a common genetic relationship, as in the case of the Vesta clan (Binzel and Xu 1993). The most reliable families identified by means of statistical techniques can provide essential information on the physical characteristics of the impacts responsible for their formation. In particular, from the point of view of the physics of catastrophic collisions, asteroid families are the outcome of experiments that Nature performed in ranges of masses and impact energies which are far beyond those obtainable in our laboratories. This is very important, taking into account that this branch of the physics is presently not very well understood, in spite of its importance in many fields of planetary research. The study of asteroid families can provide information on the size, shape, ejection velocity, and spin rate distributions of the fragments originating from collisions among objects of asteroidal sizes, from some tens up to some hundreds of kilometers These data, in turn, should be compared with the predictions of the most recent attempts of modeling collisional breakup phenomena: those based on a hydrocode approach (Melosh *et al.* 1992, Benz and Asphaug 1994, Benz *et al.* 1994) and those based on a semiempirical approach (Paolicchi *et al.* 1989, 1993, 1994; Verlicchi *et al.* 1994). However, any analysis aimed at extracting from the observational data direct information on the original events of family formation should take into account all of the possible evolutionary processes which have possibly affected the family structure since its origin.

Such processes should be mainly of two kinds: collisional evolution processes and dynamical processes. The former are easily understandable, taking into account that the newly formed members of any given family must take part in the general process of collisional evolution of the asteroid belt. This leads to the collisional disruption and gradual erosion of the family members, the smallest being lost in shorter time scales. These kinds of processes have been recently quantitatively studied by Marzari *et al.* (1995). Of course, collisional evolution mechanisms act over long time scales and are noticeably independent on the site of family formation within the asteroid main belt. On the other hand, dynamical processes are more strongly dependent upon the family location, on the basis of the overall dynamical structure of the asteroid belt. In turn, this is in general determined by the location of the main mean motion and secular resonances.

To understand whether a given family is affected by a secular resonance is quite simple, since the locations of family members and secular resonances are usually represented in the same space, namely that of orbital *proper elements*; on this subject a large amount of work has been performed by Milani and Knežević (1990, 1992, 1994). Conversely, the relationship between families and mean motion resonances is much more complicated and is still mostly unexplored. Two main features characterize the secular dynamics close to a mean motion resonance: a secular oscillation of the asteroid elements and a secular *pulsation* of the resonance itself. These two phenomena interplay and can lead to possible adiabatic captures of family members into the resonance. All of this must be taken into account in the definition of new resonant proper elements, allowing us to perform correctly the comparison between the location of the family and the location and the width of the mean motion resonance. These new proper elements correspond to the minimal distance from the resonance's border that any member can reach during its dynamical evolution.

Section 2 is pure celestial mechanics and is devoted to explaining in detail the dynamics of bodies close to mean motion resonances and to defining the new resonant proper elements that we use afterward to discuss the structures of the main families.

Section 3 describes our model of isotropic disruption of the parent body of an asteroid family. We construct the curves which describe the location in the orbital elements space of the fragments isotropically ejected with a given velocity. We use these curves in order to check if families could have injected fragments into the nearby mean motion resonances.

In the further sections we use all of the tools developed in sections 2 and 3 to investigate the dynamical effects of mean motion resonances on some of the most important families of the asteroid belt. Section 4 is devoted to the family of Themis and section 5 to the family of Eos. Section 6 describes the case of the quasi-isotropic families of Adeona, Dora, and Gefion (Ceres). Finally, section 7 concerns the nonisotropic families of Eunomia, Maria, Nysa, and Hygiea. The family of Koronis is not analyzed in the present paper, since the theory of adiabatic secular capture into mean motion resonances, explained in section 2, cannot be applied in this particular case.

The data concerning the number and identity of the family members are those obtained by means of the hierarchical clustering method, developed by Zappalà *et al.* (1990) and updated by Zappalà *et al.* (1994, 1995). We could have used as well the data coming from the wavelet analysis method (WAM), developed by Bendjoya *et al.* (1991). Indeed, as pointed out by Zappalà *et al.* (1995), the results obtained by means of these two methods are in general in very good agreement, with all differences

being of scarce importance for the purposes of the present paper.

2. DYNAMICS OF BODIES CLOSE TO MEAN MOTION RESONANCES

Since the original works of Wisdom (1983, 1985), many astronomers conjectured that mean motion resonances can be routes of meteorite transport (see Greenberg and Nolan, 1989). According to this scenario, the fragments produced in asteroid collisions which happen to fall into a mean motion resonance have the eccentricity pumped up to Mars and Earth-crossing values. Farinella *et al.* (1993) showed that many asteroids in the main belt are close enough to some mean motion resonance to inject there a significant fraction of fragments, in case of breakups. (Most of) the asteroids analyzed in that paper, however, are not the parent bodies of any known asteroid family, so that during the history of the Solar System they probably have suffered only cratering collisions, producing just relatively small fragments.

Conversely, asteroid families represent the outcomes of energetic breakups producing swarms of sizable fragments. So, if we prove that families have "put" fragments into mean motion resonances, then we can be confident that such events have been the sources of important fluxes of meteoritic material to the inner regions of the Solar System We strongly suggest, therefore, that the giant impactors, such as the one which possibly caused the extinction of dinosaurs, and the biggest Earth-crossers, such as the asteroids 433 Eros and 1036 Ganymede, should have been original members of some asteroid family. Indeed, if one believes that they have been generated in a shattering event, fragments of this relatively large size ($D > 10$ km) should have been produced only in very energetic events leading to the formation of observable families.

Therefore, we need to understand properly how family fragments can be "put" into a mean motion resonance. Fragments can either be directly injected into a resonance at the time of the parent body breakup or be subsequently captured by it. This second phenomenon, i.e., an adiabatic process of capture into resonance, is most efficient since it also concerns fragments which have not directly been injected into the resonance at the time of breakup.

The ellipticity of Jupiter's orbit induces secular variations of the asteroidal eccentricities and modulates the width of the libration zone in a mean motion resonance. An animated view in the (a, e) plane would essentially show an up and down motion of the asteroid coupled with a pulsation of the V-shaped borders of the resonance (a sort of symmetric accordion-like motion). The two phenomena are in phase, being produced by the same cause, and this allows a repartition of family members into two classes: resonance-crossers and non-resonance-crossers. We stress that surviving family members belong to the second class. Asteroids of the first class, on the contrary, have periodically encountered the resonance separatrix and we conjecture that they have been sooner or later captured into the resonance and subsequently ejected from it or, at least, lost as far as their identification as family members is concerned.

In Fig. 1, we show the typical behavior of an asteroid belonging to the 5/2 resonance-crossers class. There, the averaged equations of the restricted three-body problem Sun–Jupiter–asteroid are integrated with the aid of the well-known Schubart integrator (Schubart, 1978). As shown in Fig 1, the asteroid jumps from one side of the resonance to the other side with temporary captures into

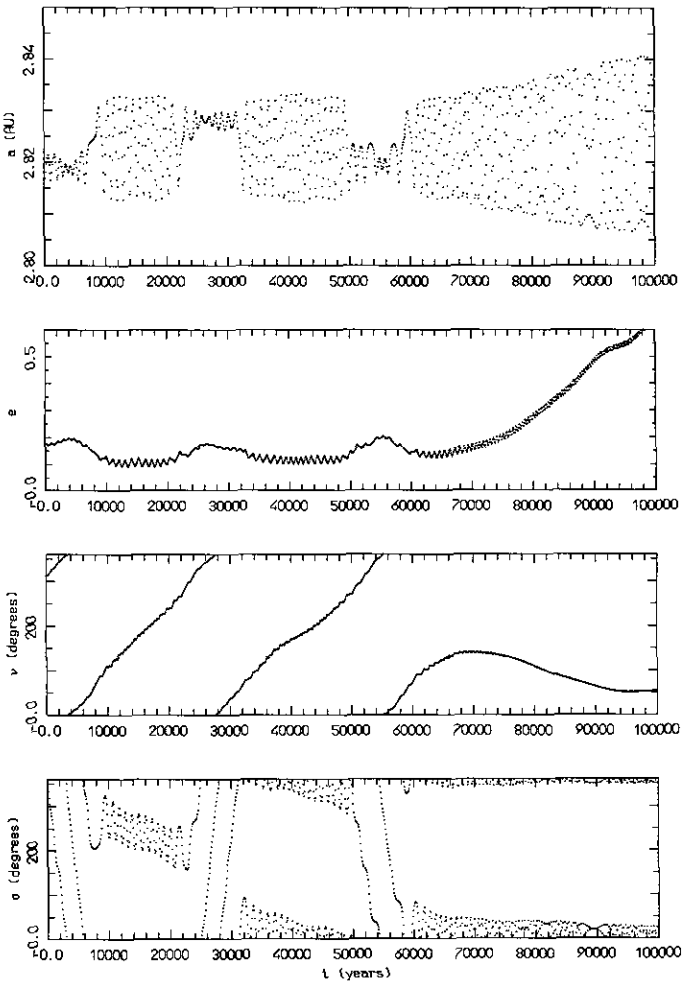

FIG. 1. Averaged numerical integration near the 5/2 mean motion resonance within the framework of the elliptic restricted three-body problem. Here ν denotes $\tilde{\omega} - \tilde{\omega}'$, with $\tilde{\omega}'$ being the longitude of perihelion of the perturbing planet. The angle σ is the critical angle of the 5/2 resonance, i.e., $\sigma = 5/3\ \lambda' - 2/3\ \lambda - \tilde{\omega}$. The initial conditions are: $a = 2.818$ AU, $e = 0.17673$, $i = 9.5348°$, $\omega = 319.13°$, $\Omega = 352.78°$, and $\sigma = -353.22°$. See text for comments.

resonance. At $t \sim 6 \times 10^4$y, it finally enters the 5/2 resonance in the corotation zone, i.e., in the region where $\tilde{\omega} - \tilde{\omega}'$ librates. The secular libration of $\tilde{\omega} - \tilde{\omega}'$ in the 5/2 resonance pumps the eccentricity up to Earth-crossing values. Within the framework of the restricted three-body problem, however, the global behavior is relatively regular. This regular character disappears as soon as we perform the integration in a more realistic model taking account of the secular variations of Jupiter's orbit. In that case, once captured, the asteroid undergoes strong perturbations due to the overlapping secular resonances (Morbidelli and Moons 1993, 1995; Moons and Morbidelli 1995).

In order to highlight the feasibility of the capture process, we have to define a feasible way for representing the asteroid families and the nearby resonances at the same time. This is done by plotting the location of the surviving family members and of the nearby resonance borders at their position of closest approach. This defines what we call the *resonant proper elements*. The results are presented in the next sections and are convincing: several families seem to be cut by resonances, the family borders coinciding with the delimitation of the resonance zones; in other words, families did "put" members into mean motion resonances associated with Kirkwood gaps. The remainder of the section will be devoted to theoretical explanations and technical details of computation. The pulsation of the resonances is explained first. The motion of asteroids is then analyzed and conditions of closest approach are determined. Finally, the way of computing the minimum distance to the resonance for each asteroid as well as the way of presenting the results is explained in detail.

2.1. *Pulsation of Resonances*

After an averaging of the short periodic variations of the orbital elements associated with the revolution of the asteroid around the Sun, the dynamics close to a mean motion resonance are usually characterized by two distinct time scales. The shorter one concerns the oscillation of (mainly) the semi-major axis associated with the motion (libration or circulation) of the critical angle of the resonance. The longer one concerns the secular oscillation of (mainly) the eccentricity due to the ellipticity of Jupiter's orbit.

Within the framework of the circular problem (i.e., neglecting the eccentricity of Jupiter), the long periodic secular oscillations disappear and the averaged resonant problem is integrable. The dynamics of a $(p + q)/p$ mean motion resonance can be described by pendulum-like pictures, such as those in Fig. 2. The variables in these pictures are the angle $q\sigma$ and the semi-major axis a, with σ being the critical angle of the resonance

$$\sigma = \frac{p+q}{q}\lambda' - \frac{p}{q}\lambda - \tilde{\omega}, \qquad (1)$$

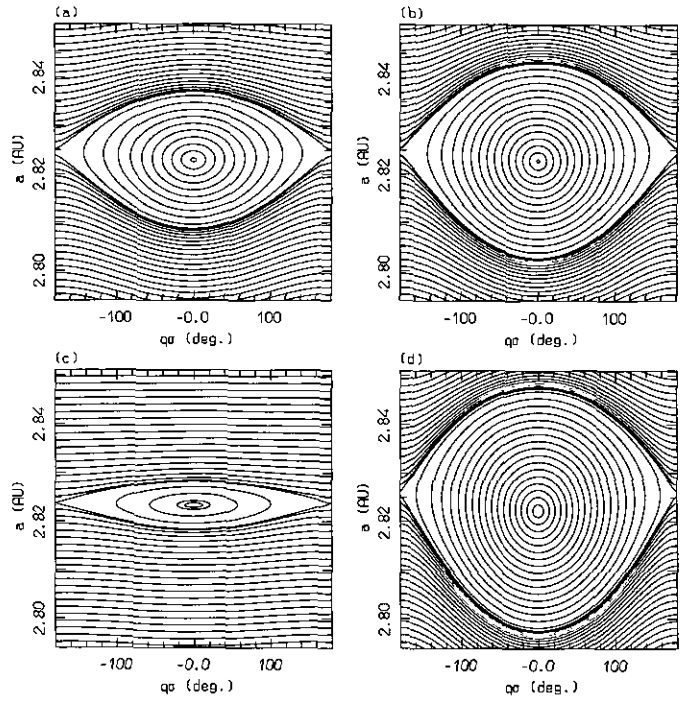

FIG. 2. Dynamics in the 5/2 mean motion commensurability. (a and b) Computed for $e' = 0$ and two different values of the asteroidal eccentricity at the libration center: 0.204 (a) and 0.26 (b). (c and d) Computed for $e' = 0.05989$, an asteroidal eccentricity 0.204 at the libration center, and two different values of $\tilde{\omega} - \tilde{\omega}'$: 0 (c) and π (d).

where λ is the mean longitude of the asteroid and $\tilde{\omega}$ is the asteroid's longitude of perihelion (primed notations refer to Jupiter). The dynamical picture is characterized by the existence of a "cat's eye"-shaped region where $q\sigma$ librates, delimited by critical curves called the separatrices. The separatrices cut the vertical axis passing through the center of libration in two points with semi-major axes $a_{\min}$ and $a_{\max}$. The resonance width can be defined as the distance between these two points. As seen in Figs. 2a and 2b, the resonance width increases with increasing value of the eccentricity at the center of libration, and therefore $a_{\min}$ and $a_{\max}$ depend on this eccentricity. If we record their values for all eccentricities on a diagram in the (a, e) space, we find that the borders of the mean motion resonance have a typical V-shaped form (see, for instance, Henrard and Lemaitre 1983a; Dermott and Murray 1983; and Lemaitre 1984, for more details on mean motion resonances in the planar circular restricted problem).

Taking into account the eccentricity of Jupiter's orbit, the problem is no longer integrable. Nevertheless, since in most of the cases (with the exception of the Koronis family) the time scales concerning the mean motion resonance and the secular oscillations are well separated, one can still describe the dynamics by the same model, depending adiabatically on the secular angle $\tilde{\omega} - \tilde{\omega}'$.

Figure 2 also shows the resonant dynamics for $\tilde{\omega} - \tilde{\omega}' = 0$ (c) and $\tilde{\omega} - \tilde{\omega}' = \pi$ (d) for the same value of the eccentricity at the libration center as in Fig. 2a. We remark that the resonant width changes with $\tilde{\omega} - \tilde{\omega}'$ (see also Yoshikawa 1990, 1991), which can be understood as follows. The resonance width for $(p + q)/p$ mean motion commensurability is directly proportional to the leading resonant term $\alpha_q e^q \cos(q\sigma)$ of the disturbing function, with this term being evaluated at the libration center (Malhotra 1994). In the elliptic case, different contributions to the leading term in the averaged disturbing function arise which are of the form

$$\alpha_q e^q \cos(q\sigma) + \sum_{j=0}^{q-1} \alpha_j e^j e'^{q-j} \cos[q\sigma + (q-j)(\tilde{\omega} - \tilde{\omega}')]. \tag{2}$$

The coefficients $\alpha_j (0 \leq j \leq q)$, which are functions of the ratio in averaged semi-major axes between the asteroid and Jupiter, alternate in sign and, hence, all contributions to the term in $\cos(q\sigma)$ accumulate when $\tilde{\omega} - \tilde{\omega}' = \pi$ because they are all of the same sign. Within the framework of the elliptic restricted three-body problem (e' and $\tilde{\omega}'$ fixed), the resonance width is thus maximum for $\tilde{\omega} - \tilde{\omega}' = \pi$ and minimum for $\tilde{\omega} - \tilde{\omega}' = 0$.

In order to get a realistic model, the variations of Jupiter's orbit under the influence of Saturn must be taken into account. Following the synthetic theory LONGSTOP1B (Nobili *et al.* 1989), the most important terms describing the behavior of Jupiter's eccentricity and longitude of perihelion are

$$\begin{aligned} e' \cos\tilde{\omega}' &= m_{5,5} \cos(g_5 t + \tilde{\omega}_5^0) + m_{5,6} \cos(g_6 t + \tilde{\omega}_6^0) \\ e' \sin\tilde{\omega}' &= m_{5,5} \sin(g_5 t + \tilde{\omega}_5^0) + m_{5,6} \sin(g_6 t + \tilde{\omega}_6^0), \end{aligned} \tag{3}$$

with $m_{5,5} = 4.419 \times 10^{-2}$, $m_{5,6} = -1.570 \times 10^{-2}$, $g_5 = 4.2575''/y$, $g_6 = 28.2455''/y$, $\tilde{\omega}_5^0 = 27.0°$, $\tilde{\omega}_6^0 = 124.2°$.

The absolute maximum width will thus be obtained for $\tilde{\omega} - \tilde{\omega}_J = \tilde{\omega} - g_5 t - \tilde{\omega}_5^0 = \pi$ and $\tilde{\omega} - \tilde{\omega}_S = \tilde{\omega} - g_6 t - \tilde{\omega}_6^0 = 0$ as, in that case, $e' = 5.989 \times 10^{-2}$ (its maximum value) and $\tilde{\omega} - \tilde{\omega}' = \pi$. Conversely, the absolute minimum width corresponds to $\tilde{\omega} - \tilde{\omega}_J = 0$ and $\tilde{\omega} - \tilde{\omega}_S = \pi$ where $e' = 5.989 \times 10^{-2}$ and $\tilde{\omega} - \tilde{\omega}' = 0$. As an example, Fig. 3 shows the V-shaped traces of the maximal and minimal separatrices in the case of the 5/2 mean motion commensurability.

It is important to notice that, even within the framework of the elliptic restricted problem (i.e., when e' and $\tilde{\omega}'$ are considered as constants), the resonance width is a function of $\tilde{\omega}$ and, hence, varies from asteroid to asteroid. Therefore, we can conclude that each asteroid "sees its own resonance." However, this is not a problem for the purposes of the present study. Indeed, in order to obtain a clear picture of the interaction between a family and a resonance, it will be sufficient to consider each family member at the time of its closest approach with the resonance border.

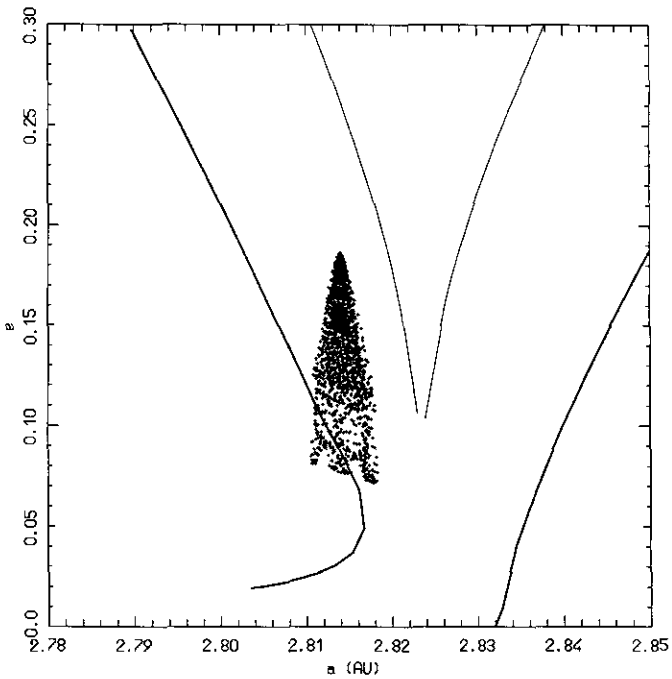

FIG. 3. Averaged numerical integration near the 5/2 mean motion resonance taking into account the secular variations of Jupiter's orbit. See text for comments. The initial conditions are: $a = 2.815$AU, $e = 0.15673$, $i = 9.5348°$, $\omega = 319.13°$, $\Omega = 352.78°$, and $\sigma = -353.22°$. The separatrices of the 5/2 are plotted for the maximum and the minimum value of the resonance width (bold lines and thin lines, respectively).

2.2. *Conditions of Closest Approach*

Interestingly enough, closest approaches between family members and nearby resonances do not necessarily occur when the asteroid is at a maximum eccentricity nor when the resonance width is maximal. To understand this, closest approaches with a given mean motion resonance can easily be identified by looking at asteroid semi-major axis behavior as shown in Fig. 2: the more a varies, the closer is the resonance. Figure 3, for instance, shows the results of an averaged numerical integration of a member of the Gefion family, at the border of the 5/2 resonance. Results are plotted in the (a, e) plane of semi-mean elements associated to the 5/2, i.e., averaged elements obtained by averaging out all terms in λ' except the resonant one $5\lambda' - 2\lambda$. The semi-mean elements are plotted every 100 years. During this integration, the asteroid goes up and down slowly (secular variation in eccentricity) while performing a series of almost horizontal oscillations (variations in semi-major axis due to the proximity of the mean motion resonance).

The cone-like shape of the result indicates that the maximal amplitude of oscillation in semi-major axis or, in other words, the maximum deformation of the orbit for one period in σ, occurs when the eccentricity is at the minimum of its secular oscillation.

The families of Dora, Adeona, Eunomia, and Eos have the same behavior as the Gefion family, i.e., for each member, the amplitude of oscillation of the semi-mean a is maximal when e is at its minimal value. The minimum of e is obtained when $\tilde{\omega} - \tilde{\omega}_J = \pi$ and $\tilde{\omega} - \tilde{\omega}_S = 0$ and, at this configuration, the corresponding resonance width is maximal. In the cases of these families, therefore, the dependence of the resonance width upon the secular angles is dominating with respect to its dependence upon the asteroid's eccentricity.

For the Themis and Hygiea families, the closest approach between an asteroid and the 2/1 resonance border occurs for $\tilde{\omega} - \tilde{\omega}_J = 0$ and $\tilde{\omega} - \tilde{\omega}_S = \pi$. At this time, the asteroid eccentricity is at the maximum of its secular oscillation and the resonance width is minimal.

Finally, closest approach between the Maria and Nysa families and the border of 3/1 mean motion resonance occurs for $\tilde{\omega} - \tilde{\omega}_J = \tilde{\omega} - \tilde{\omega}_S = \pi$. This corresponds to an intermediate value of the secular oscillation in eccentricity and to an intermediate value of the resonance width as e' is minimum and $\tilde{\omega} - \tilde{\omega}' = \pi$.

We stress that the determination of the closest approach conditions is only based here on the values of $\tilde{\omega} - \tilde{\omega}_J$ and $\tilde{\omega} - \tilde{\omega}_S$ and does not take into account the inclination nor the high order terms in the secular theory of Jupiter. A more complete theory could be made, of course, but this goes beyond the scope of the present paper. This simple version of the theory, indeed, allows us to get enough accurate results on the relative location of asteroid families and mean motion resonances.

2.3. *Computation of the Resonant Proper Elements*

In order to compare the location of the resonance separatrices with the location of the nearby family members, we have to adopt a compatible way of representing both, which is given by the so-called *resonant proper elements*. More precisely, we proceed as follows:

- first, we plot in the (a, e) plane the traces of the resonance separatrices computed for the values of e' and $\tilde{\omega} - \tilde{\omega}'$ which give closest approach (see previous subsection) to the neighboring families;
- second, we determine the resonant proper semi-major axis and eccentricity for each family member and plot each of them at the corresponding location in the (a, e) plane.

In what follows, we shall adopt the notations (a_P, e_P) for the proper (a, e) and (a_R, e_R) for the resonant proper (a, e).

The resonant proper eccentricity e_R is defined as the value of the semi-mean e at the time of closest approach with the resonance border. Knowing the values of $\tilde{\omega} - \tilde{\omega}_J$ and $\tilde{\omega} - \tilde{\omega}_S$ for which closest approach occur (see previous subsection), we can follow the averaged motion of the asteroid up to the corresponding time and determine the value of the semi-mean e at that time: this gives the resonant proper eccentricity.

The resonant proper semi-major axis a_R is defined as the value of the semi-mean a when the semi-mean $e = e_R$ and when σ has the value corresponding to the libration equilibrium. We recall (see subsection 2.1) that the V-shaped form of the separatrices in the (a, e) plane is obtained by plotting, for each value of eccentricity at the libration center, the intersections a_{min} (left branch) and a_{max} (right branch) of the separatrices with the vertical axis passing through the libration center. If we want to represent asteroids in a compatible way with resonances, we have to plot both not only for the same value of e' and $\tilde{\omega} - \tilde{\omega}'$, but also for the same value of σ. Having followed the averaged motion of the asteroid up to the time of closest approach with the resonance border, we can then look at the semi-mean a over one period in σ and determine its value when σ equals 0 (for the 2/1, 9/4, 5/2, and 8/3 mean motion commensurabilities), when σ equals $\pi/4$ (for the 7/3 mean motion commensurability), or when σ equals $\pi/2$ (for the 3/1 mean motion commensurability): this gives the resonant proper semi-major axis.

The computation of the resonant proper (a, e) for near-resonant asteroids could be done by numerically integrating their orbit up to the point of closest approach. Nevertheless, some of the families are very populated and this would result in a great amount of manipulations. With reasonable approximations, however, some shortcuts can be taken which considerably simplify the procedure:

1. Taking account of the relative compactness of asteroid families in the proper elements space, we can assume (and the validity of this hypothesis has been checked) that the eccentricity repartition about the parent body is conserved in the resonant proper space. As a consequence, we proceed as follows for each family:

- With a realistic numerical integration we determine e_R for the parent body. This is done by integrating the equations of motion of the parent body over 3×10^5 years, using a Bulirsh-Stoer variable step size integrator (Stoer and Bulirsh 1980) and taking the perturbations of the four giant planets into account
- Denoting $\Delta e = e_P - e_R$ for the parent body, we subtract Δe from the value of e_P of each family member in order to get its e_R.

Obviously, this shortcut can only be taken when the proper eccentricity is greater than the forced one, otherwise we would end with a negative resonant proper eccentricity.

This is another reason for preventing the study of the Koronis family.

2. In most cases, the single computation of e_R is sufficient and we can set $a_R = a_P$ with a good approximation. Indeed, even if the effect of a nearby mean motion resonance does more or less affect a large number of family members, this effect is very small as soon as we move off a little bit from the resonance. In that case, as the semi-mean a is almost constant, we do not compute its exact value for the value of σ at the libration center but we proceed as follows:

• If the point (a_P, e_R) is sufficiently distant from the resonance border (computed at the time of closest approach), we define the resonant proper elements as (a_P, e_R), i.e., we set $a_R = a_P$.

3. For asteroids near the resonance border, however, it is important to compute the exact a_R. Indeed, a_P is, in that case, a very bad approximation of the resonant proper value of a: sometimes it would even locate a near-resonant asteroid *inside* of the resonance! This is the case, for instance, for the asteroid in Fig. 3: this asteroid is outside of the resonance but, as the values of the semi-mean (a, e) have been plotted regardless of the value of the critical angle σ, it seems to cross the resonance border. On a cat's eyes diagram like those in Fig. 2, this asteroid would follow a curve located just below the lowest separatrix. The resonant proper a, i.e., the value of the semi-mean a at $\sigma = 0$, is in that case the minimum value of the semi-mean a over one period in σ when the eccentricity has the resonant proper value. For the asteroid in Fig. 3, this corresponds to the value of the semi-mean a at the left bottom corner of the cone.

In that case, we proceed as follows:

If the point (a_P, e_R) is near the resonance border or between the resonance borders (computed at the time of closest approach), we integrate the averaged equations of motion in order to find the outermost value of the semi-mean a with respect to the resonance zone at the time of closest approach. This integration is done with the ESA program (Moons 1994), which is an extension of the well known Schubart integrator and takes the secular variations of Jupiter's orbit into account (the exact terms used in this study are given in subsection 2.1). The initial semi-mean conditions of integration are computed from the osculating elements by a modified version of the program for the computation of the asteroidal mean elements (Milani and Knežević 1990)

3. ISOTROPIC DISRUPTION MODEL FOR THE DISTRIBUTION OF FAMILY MEMBERS

It is generally believed that all of the asteroid families originated from the breakup and shattering of single parent bodies due to high velocity inter-asteroidal collisions (at mean velocities of the order of 5–6 km/sec: see Farinella and Davis 1992; Bottke *et al.* 1994). The resulting distributions of the fragments in the space of the orbital elements exhibit in several cases a highly complex appearance. This can be due to a number of reasons, including the physical and geometric properties of the original impact as well as the subsequent dynamical and physical evolution of the whole structure. For the purposes of the present paper, which is not aimed at making a detailed physical study of the families, it can be sufficient to limit the analysis to the simplest conceptual case, i.e., a breakup producing a swarm of fragments ejected *isotropically*. This exercise would allow us to obtain a simple model of the expected structure of the families, which, when compared with the real cases, can help in assessing the effects due to the presence of external perturbing sources, like the proximity of mean motion resonances with Jupiter. This kind of approach can be considered as a first step of a detailed analysis of the kinematical structures of the asteroid families and allows us to check the effectiveness of any modeling attempt based on the simple hypothesis of an isotropic ejection of the fragments.

A simple and efficient starting point for obtaining the necessary model is offered by the well-known Gauss formulae, which give the change in the osculating orbital elements due to an impulsive change in velocity δV

$$\begin{cases} \delta a/a = \dfrac{2}{na(1-e^2)^{1/2}}\left[(1+e\cos f)\,\delta V_T + (e\sin f)\,\delta V_R\right] & (4) \\ \delta e = \dfrac{(1-e^2)^{1/2}}{na}\left[\dfrac{e+2\cos f+e\cos^2 f}{1+e\cos f}\,\delta V_T + (\sin f)\,\delta V_R\right] & (5) \\ \delta i = \dfrac{(1-e^2)^{1/2}}{na}\dfrac{\cos(\omega+f)}{1+e\cos f}\,\delta V_W, & (6) \end{cases}$$

where a, e and i are the orbital semi-major axis, eccentricity, and inclination, respectively; na is the mean orbital velocity; $(\delta V_T, \delta V_R, \delta V_W)$ are the components of δV along the direction of the motion, in the radial direction, and perpendicular to the orbital plane, respectively. The formulae contain also the two angles f (true anomaly) and ω (argument of the perihelion) at the instant of the velocity change (impact). In principle, the knowledge of the true anomaly at the instant of the impact would allow us to represent the distribution of the fragments in the (a, e) plane. Similar considerations can be made concerning the (a, i) plane, where in addition the angle $\omega + f$ has to be taken into account. In practice, the angles are unknown. However, by assuming an isotropic fragmentation, it is simple to describe the relationships e vs a and i vs a for a given value of the module of the ejection velocity V_0, and for any values of the unknown angles f and $\omega + f$. The equivelocity curves (EVCs) obtained in this way contain in the (a, e)

and (a, i) planes all of the fragments ejected with velocity smaller than (or equal to) V_0. From Eqs. (4) and (5) it is easy to see that the semi-major axis a and the eccentricity e are forced to follow a relationship controlled by the unknown true anomaly f of the parent body at the instant of the collision. In particular, for a true anomaly of 0° the relationship in the plane (a, e) is

$$\frac{\delta a}{a} = \left(\frac{1}{1-e}\right) \delta e.$$

For $f = 180°$ the relationship becomes

$$\frac{\delta a}{a} = -\left(\frac{1}{1+e}\right) \delta e.$$

In both cases the relation is a straight line, having an angular coefficient generally close to ±45° for typical asteroidal orbits. For these critical values of f, in the (a, e) plane, all of the fragments are forced to be located along a line, with the exact position depending only upon the value of the δV_T component. Obviously, the behavior corresponding to other values of f is more complicated, since in this case both the components δV_T and δV_R of the ejection velocity of each fragment determine the resulting $\delta a/a$ and δe. Let us compute the EVCs corresponding to a swarm of fragments ejected isotropically ($\delta V_T = \delta V_R = \delta V_W$). In particular, for increasingly higher values of f, it is easy to see that in the (a, e) plane we have curves similar to ellipses with increasingly larger minor axes and inclined at decreasing angles with respect to the a axis, up to an extreme value that is reached for $f = 90°$ (or $f = 270°$). Figure 4 shows the resulting curves in the (a, e) plane for f ranging from 0° to 180°. In the (a, i) plane quasi-ellipse curves are also obtained, which, however, have their major axis parallel to the a axis; the minor axis varies as a function of the $\omega + f$ angle (see Fig. 5).

In order to check if a given family can be the outcome of a quasi-isotropic breakup, we try to fit its distribution on the (a, e) and (a, i) planes with EVCs computed for several values of V_0, f, and $\omega + f$. If we find a set of values V_0, f, and $\omega + f$ with a good fit, we obtain important information about the true anomaly and the argument of perihelion at the instant of breakup and about the ejection velocity of the observed fragments. Conversely, if no EVC fits the distribution of the family well, we derive strong indications about the degree of anisotropy of the original ejection velocity field of the fragments. For the purposes of the present paper, however, we make use of the EVCs mainly to derive an approximate estimate of the number of fragments (if any) possibly ejected into nearby mean motion resonances with Jupiter. This is an obvious prerequisite of any detailed analysis of the physical properties of the events responsible for family formation.

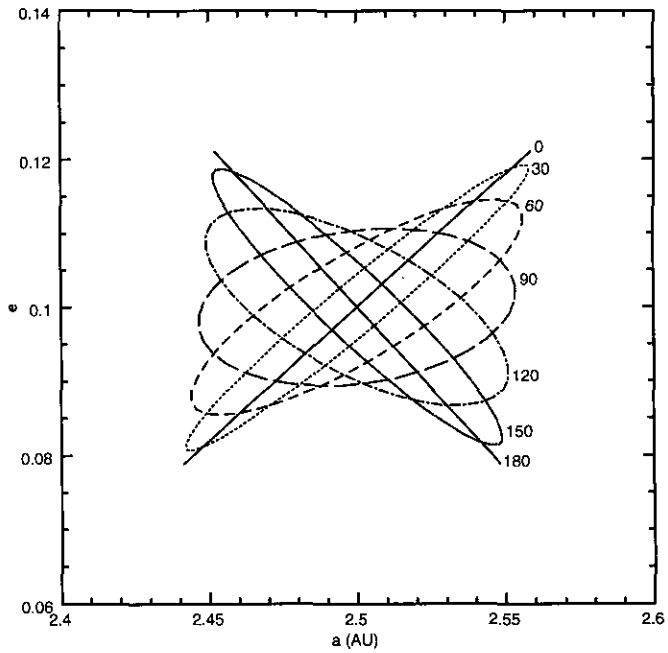

FIG. 4. Equivelocity curves in the (a, e) plane for a fictitious family having the barycentre at $a = 2.5$ AU, $e = 0.1$ and $i = 10°$, and assuming $V_0 = 100$ m/sec. Different curves correspond to values of the true anomaly f ranging from 0 to 180°.

It should be noted here that the transformation from the osculating elements space to the proper elements space

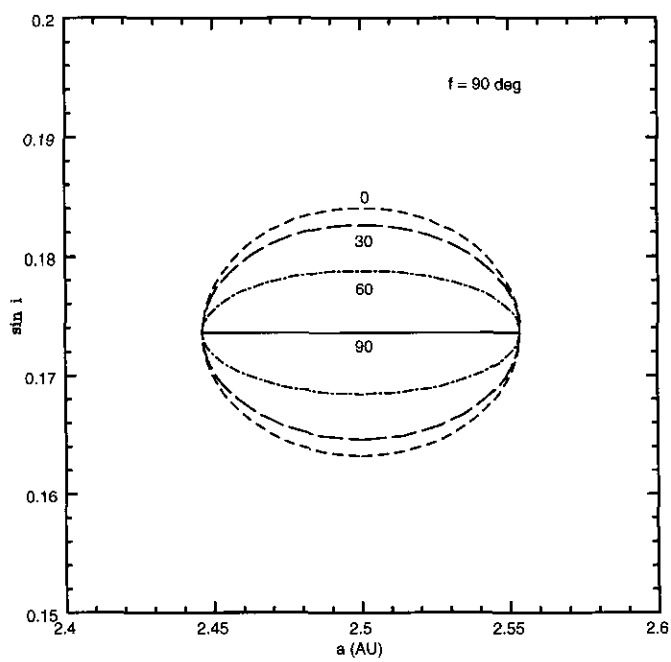

FIG. 5. The same as Fig. 4, but in the $(a, \sin i)$ plane for a true anomaly $f = 90°$ and for $\omega + f$ ranging from 0 to 90°.

can be considered "transparent" for the present purposes, since the three-dimensional structure of a family is conserved in the transformation. This has been proved to be true by Brouwer (1951) in the framework of the linear theory of the perturbations. More recently, this has also been checked by means of numerical simulations performed by Bendjoya *et al.* (1993), using the proper elements computation techniques developed by Milani and Knežević (1990, 1992). This ensures that we can draw our EVCs directly in the space of the proper elements, where the families are defined.

At the same time, some information can be inferred on the plausible sizes of the objects injected into the resonances. In fact, we recall that the results of laboratory experiments (see Fujiwara *et al.* 1989, for a review) have evidenced a relationship between ejection velocity and fragment mass, in the sense that smaller fragments are ejected at higher velocities. Such a relationship is also predicted by the most recent modeling attempts (see, e.g., Paolicchi *et al.* 1993, 1994; Melosh *et al.*, 1992, Benz *et al.*, 1994).

This means that an EVC computed for a given value of the module of the ejection velocity may be roughly associated with a certain size limit. In order to demonstrate the importance of this effect, we make use of histograms describing the distribution of the members of a given family with respect to the semi-major axis, where different size ranges are considered separately. The diameters, when not included in the IRAS output list (Tedesco *et al.* 1992), are computed on the basis of the average albedo of the family. The results confirm the existence of a velocity-sized relationship.

We shall see in the following that, having taken into account the possible fractions of members injected into mean motion resonances and subsequently lost, some families can be roughly fitted by a simple isotropic model (Dora, Gefion, Adeona), while others cannot be fitted at all (Eos, Themis). For some of them (Maria, Eunomia) no definitive conclusions can be obtained with the present data. Other more complex structures, like Nysa, are very probably connected with multiple events, while the large Koronis family is not analyzed in the present paper, even if its interaction with some mean motion resonances is surely not negligible (see Milani and Farinella 1995). These more complex cases will be studied in detail in subsequent papers together with a more physical interpretation of all of the most prominent families. Finally, the family of Hygiea represents a typical outcome of an energetic cratering event for which an isotropic model can *a priori* be ruled out.

4. THE THEMIS FAMILY

The Themis family is a huge one. Its parent body should have been about 300 km in size, as can be deduced by adding together all of the masses of the currently known members. From the dynamical point of view, this family is peculiar, since it is the closest to the 2/1 mean motion resonance. This resonance corresponds to the widest Kirkwood gap in the asteroid belt, so that it is of great interest to analyze the extension of the Themis family with respect to the resonance borders.

Since the 2/1 resonance is very strong, adopting suitable resonant proper elements, as described in section 2, is particularly important. In this case the resonant proper semi-major axis and eccentricity are the values that the mean a and e assume when $\sigma = 0$, $\tilde{\omega} - \tilde{\omega}_J = 0$, and $\tilde{\omega} - \tilde{\omega}_S = \pi$; this configuration corresponds to a maximum of the eccentricity of each family member.

Using these resonant proper (a_R, e_R) coordinates, the family can be plotted together with the edges of the 2/1 resonance, as shown in Fig. 6. The result is astonishing: the rightmost bound of the family *is* the leftmost border of the 2/1 resonance. It is not believable that such a configuration can be due to chance. We must conclude that many original members of the Themis family have been adiabatically captured into the 2/1 resonance and subsequently eliminated.

This has a number of implications. The origin of the 2/1 Kirkwood gap is a long standing problem in celestial mechanics. Unlike the other mean motion resonances in the asteroid belt, all attempts, both analytical and numeri-

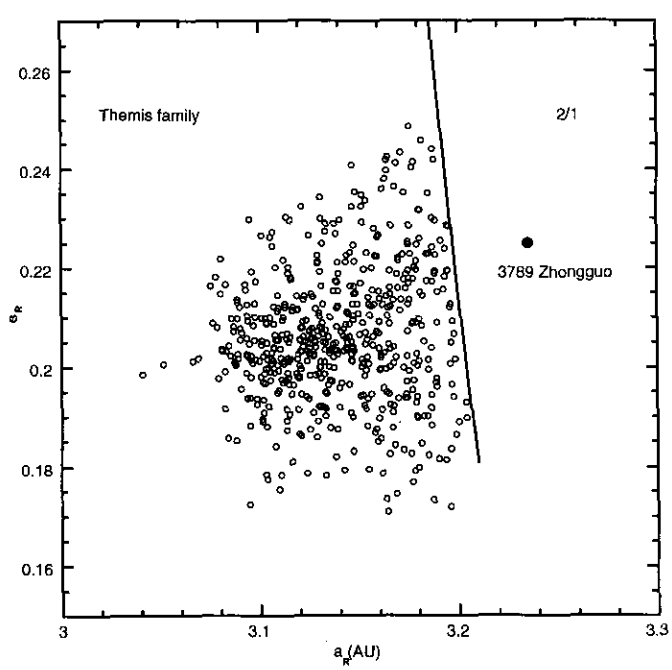

FIG. 6. The Themis family plotted in the resonant proper elements plane (a_R, e_R) together with the leftmost separatrix of the 2/1 resonance. We recall that the leftmost separatrix of the 2/1 resonance is defined only for $e_R > 0.18$ (see Morbidelli and Moons 1993). The position of the asteroid 3789 Zhongguo is also reported (see text for more details).

cal, at finding a general mechanism for depleting the 2/1 resonance have not been successful so far. The fact that the Themis family is abruptly cut at the border of the 2/1 resonance implies that, at a given time, the resonance must have been populated. Therefore, a mechanism for depletion of the 2/1 resonant region *must* exist.

Henrard and Lemaitre (1983b) proposed a mechanism of depletion which takes into account the shift of mean motion resonances in the primitive phases of the Solar System, during the dissipation of the Solar nebula. According to this scenario, resonances were moving outward, in the direction of Jupiter, and all planétesima have been ejected from the resonance during this drift. Now, the fact that the border of the Themis family coincides with the *present* leftmost border of the 2/1 resonance indicates that the disruption of the parent body occurred after the end of the resonance sweeping. Therefore, although the Henrard and Lemaitre mechanism can explain the depletion of primordial bodies near the 2/1 resonance, it cannot explain the depletion of the members of the Themis family.

The most recent and detailed study of the dynamics of the 2/1 resonance has been done by Henrard *et al.* (1995). These authors pointed out that within the 2/1 resonance there are both regions of stable motion and regions of chaotic motion with possible diffusion to large eccentricities, as in the case pointed out by Wisdom (1986). A complete and detailed map of these regions has still to be done, but it seems that the unstable regions are concentrated at moderate eccentricity and large amplitude of libration, i.e., on the ideal extrapolation of the Themis family inside the 2/1 resonance. Therefore, a possibility (to be checked by further investigations) is that the members of the Themis family have all been injected into these unstable regions and, by consequence, depleted. Nevertheless, there is the hypothetical possibility that some small fragment, ejected with higher escape velocity, could have reached a stable region and still exists, undiscovered, in the 2/1 resonance.

Interestingly, there is one asteroid with moderate eccentricity in the 2/1 resonance: 3789 Zhongguo. This object has an orbit which is in a stable island throughout the long time spans of numerical integrations (Milani, private communication). We have computed numerically the evolution of the orbit of this asteroid, using the Extended Schubart Integrator (Moons 1994), in order to compute resonant proper elements compatible with those used for the members of the Themis family and for the definition of the borders of the 2/1 resonance. Its position on the resonant proper (a_R, e_R) plane is indicated by a circle in Fig. 6. 3789 Zhongguo appears to be on the possible extrapolation of the Themis family into the 2/1 resonance. In addition the inclinations of 3789 Zhongguo and of the members of the Themis family are very similar. Therefore, it is tempting to conjecture that 3789 Zhongguo is the only known original member of the Themis family which survived into the 2/1 Kirkwood gap.

How many members of the Themis family have been captured into the 2/1 resonance and consequently lost? It is not easy to answer this question in a quantitative way. Indeed, it is not easy to explain the present structure of this family by means of a single isotropic event; in other words, it is not possible to find an equivelocity curve (see section 3) which fits the distribution of the observed family members well. Therefore, we have no tool at our disposal for making a precise estimate of the distribution and the width of the missing part of the family.

However, some conclusions can be based on the histogram of the distribution of the family members with respect to the semi-major axis (Fig. 7). Here, decreasing size limits are associated with differently shadowed parts. More exactly, the filled part of the histogram refers to objects larger than 50 km. The other, increasingly lighter, parts correspond to size limits of 30 and 20 km and to the whole sample, respectively. Note that 20 km corresponds to the expected size limit of completeness for this family (Zappalà and Cellino 1995). The vertical lines indicating the edges of the resonance are taken for values of the semi-major axis corresponding to an average value of the eccentricity

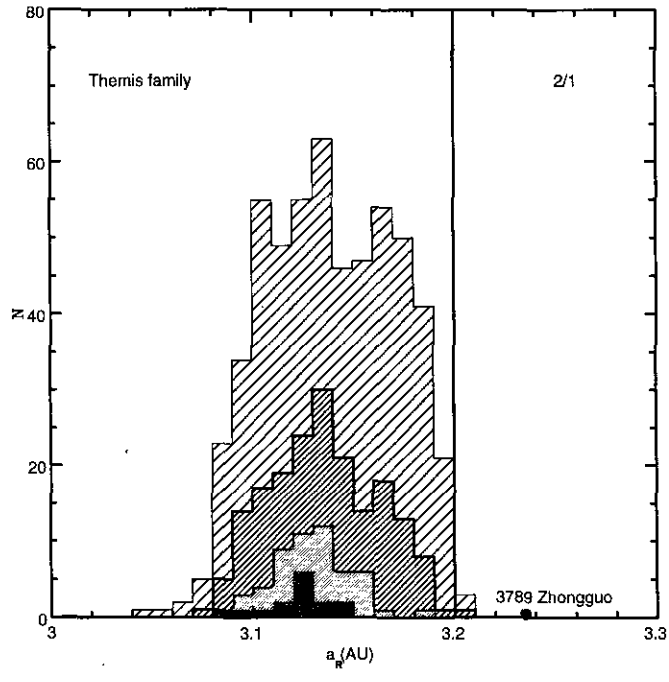

FIG. 7. Histogram of the distribution of the Themis family members with respect to the resonant proper semi-major axis. Decreasing size limits are associated with differently shaded parts. Darker to lighter parts correspond to size limits of 50, 30, and 20 km and to the whole sample, respectively. The completeness limit is 20 km. The vertical line on the right hand side denotes the inner border of the 2/1 resonance, computed for the average value of the resonant proper eccentricity of the Themis family.

of the family. This is the reason why in Fig. 7 the family seems to enter the resonance, while this is absolutely not the case (see Fig. 6). Looking closer at Fig. 7 we recognize the presence of a secondary peak located at the right side. The existence of this possible secondary event can be supported by the fact that almost all of the objects larger than 50 km are concentrated in the low a_R part (the primordial one ?) of the family. Figure 7 suggests also that objects larger than 20 km probably cannot have been ejected into the 2/1 resonance. We remark that 3789 Zhongguo, having a diameter of about 10–15 km, is located on the extrapolation of the histogram into the 2/1 resonance.

5. THE EOS FAMILY

With more than 450 members (according to Zappalà *et al.* 1995) the Eos family is the third largest family in the asteroid belt. The structure of the family is peculiar, being abruptly cut at $a \simeq 3.03$ AU into a high density part and a low density part. We have tried to correlate this sharp border between the two parts with the presence of the 9/4 mean motion resonance. Figure 8 shows the distribution of the Eos family members on the plane of resonant proper semi-major axis and eccentricity, together with the borders of the 9/4 and 7/3 resonances. The result is striking:

(i) the rightmost bound of the high density part of the family is in a very good correspondence with the left border of the 9/4 resonance;

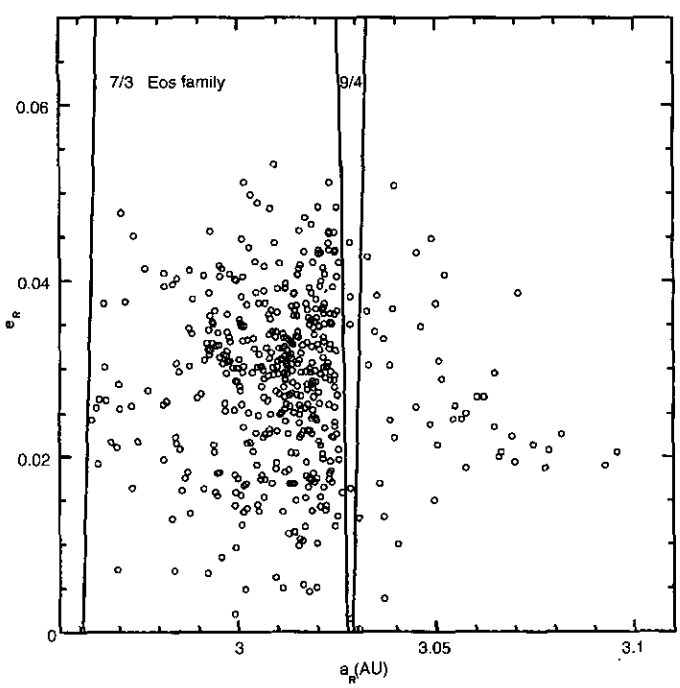

FIG. 8. The same as Fig. 6, but for the Eos family. The 7/3 and 9/4 resonances are indicated.

(ii) the low density part of the family is at the right hand side of the 9/4 resonance;

(iii) five members of the Eos family are currently inside the 9/4 resonance (this feature is unique among the currently known asteroid families and resonances);

(iv) the left border of the Eos family seems to be connected with the border of the 7/3 resonance.

At this point some caution is necessary. The resonant proper elements with respect to the 9/4 resonance that we have introduced correspond to the values assumed by the semi-mean a and e when $\sigma = 0$, $\tilde{\omega} - \tilde{\omega}_J = \pi$, and $\tilde{\omega} - \tilde{\omega}_S = 0$. Such a configuration corresponds to the phase of minimal eccentricity of each member of the family with respect to the oscillations with argument $\tilde{\omega} - \tilde{\omega}_J$ and $\tilde{\omega} - \tilde{\omega}_S$. In this computation, we have neglected the effects of the secondary resonant term with the argument $\tilde{\omega} + \Omega - \tilde{\omega}_S - \Omega_S$, which also acts slightly on the eccentricity. Since the borders of the 9/4 resonance are almost vertical lines in the (a_R, e_R) plane, we do not believe that this neglected term would change significatively our results on the location of the family members with respect to the 9/4 resonance. Nevertheless, we have integrated numerically the full equations of motion of the asteroids in the 9/4 resonance in order to check their resonant character and verify whether the 9/4 resonance could produce some instability and diffusion in the proper elements space.

In particular, the procedure that we have adopted is the following. The five resonant objects which we have plotted for simplicity in the middle of the 9/4 resonance are: (4243) $1981GF_1$, (4381) Uenohara, (4593) $1980FV_1$, $3197T_2$, and $5104T_3$. The last two bodies have been observed during only one opposition, so that their orbital elements are uncertain. Moreover, there is one more numbered asteroid, i.e., (1588) Descamisada, which is very close to the border of the 9/4 resonance; in Fig. 8 it is represented at $e = .0004$ and $a = 3.0305$ AU. We have integrated the equations of motion of the four numbered asteroids mentioned above over 100 Myr, using a Bulirsch-Stoer variable step size integrator (Stoer and Bulirsch 1980), and taking into account the perturbations of the four giant planets. Over such a long time span the numerical integrations can no longer be considered as ephemerides of the real asteroids; however, they are very useful in revealing the dynamical nature of these bodies and show possible paths for their future evolution (see Milani and Farinella 1994). These integrations are also useful in exploring the dynamical characteristics of the 9/4 resonance, which have never been explored in detail so far.

At a first glance, the evolution of the orbit of all of the integrated bodies seems to be chaotic. None of the bodies is permanently locked into the 9/4 resonance: they all jump from one side of the resonance to the other, with only temporary trappings into the resonance. (1588) Descami-

sada is quite regular over a time span of 34 Myr; then it is suddenly captured by the 9/4 resonance and starts to behave in a much more irregular way. The eccentricity and the inclination of all of these bodies also behave chaotically, although they do not increase up to large values.

In order to compare the evolution of these bodies with respect to the size of the Eos family, we have computed the evolution of their proper elements over the integration time span. In particular, we have averaged the osculating a, e, and i of our four bodies, sampled every 2000 years, over time intervals $(t_n, t_n + 10\ \text{Myr})$, t_n ranging from 0 to 90 Myr by steps of 1 Myr. In this way we have computed "numerical proper elements" which are precise enough for our purposes; unfortunately, these elements cannot be compared directly to those computed analytically by Milani and Knežević (1990) for the members of the Eos family, since the latter are defined in a different way, so that a calibration must be applied. The calibration has been computed empirically, by comparing the numerical and the analytic proper elements over the first 1 Myr of evolution.

In Figs. 9, 10, 11, and 12 we show the evolution of the calibrated proper elements of the four bodies on the planes (a_P, i_P) and (a_P, e_P) (circles) and the distribution of the proper elements of all of the members of the Eos family (crosses).

Let's start the analysis of our results from Fig. 12. The numerical proper elements of 4593 are not constant in time. However, the elements change only very little, so

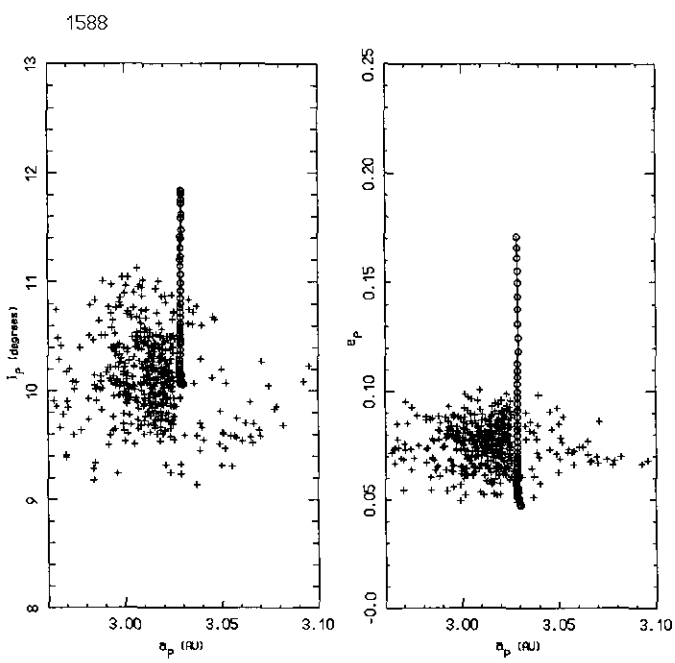

FIG. 9. The evolution of the proper elements of (1588) Descamisada over 100 Myrs (open circles) in the (a_P, i_P) and (a_P, e_P) planes. The distribution of the Eos family is also reported (crosses).

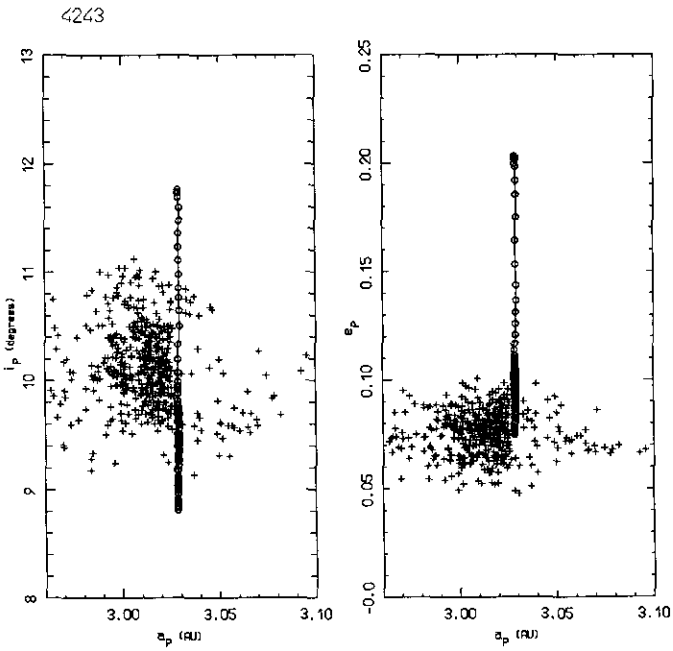

FIG. 10. The same as Fig. 9 but for the asteroid (4243) 1981GF$_1$.

that the body would be identified as a member of the Eos family over all of the 100-Myr time span. We remark that the circles are not uniformly distributed. This means that the diffusion of proper elements is not uniform, and the body can be temporarily trapped into a quasi-regular region. In particular, the proper eccentricity and inclination seem constant when the asteroid is temporarily ejected on the right-hand side of the 9/4 resonance.

The same is true for the asteroid 1588 (Fig. 9). The circles accumulate in the lower part of the (a_P, e_P) diagram since during the first 34 Myr the asteroid was on the right side of the 9/4 resonance. Then, once the body has been captured into the resonance (the semi-major axis changes a little, assuming the exact resonant value), the diffusion of e and i starts. At the end of the 100-Myr time span, the body can no longer be identified as a member of the Eos family.

In addition the asteroids 4243 and 4381 (Figs. 10 and 11) diffuse away from the family in eccentricity and/or inclination over 100 Myr.

We can draw two conclusions from these integrations. First, the 9/4 mean motion resonance is chaotic, although not strongly chaotic. In particular, the diffusion of numerical proper elements is a very slow process, unlike what is found in the cases of the stronger mean motion resonances such as 3/1, 5/2, or 7/3. Second, the members of the Eos family which are presently in the 9/4 resonance must be either very young (so that they still have not had the time to diffuse away from the family) or lucky enough to have avoided macroscopic diffusion during all of their lifetime

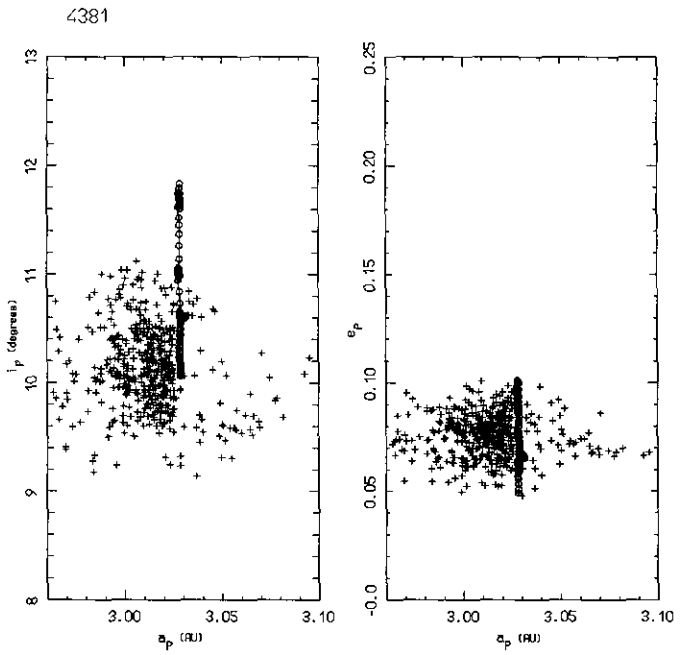

FIG. 11. The same as Fig. 9 but for the asteroid (4381) Uenohara.

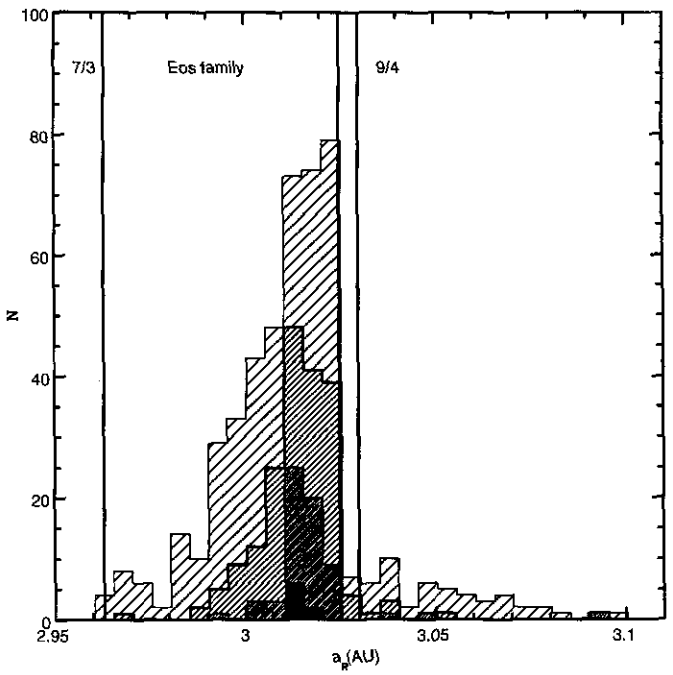

FIG. 13. The same as Fig. 7 but for the Eos family. The size limits are 40, 25, 18 and 0 (the whole sample) km. Completeness limit is 18 km. The vertical lines denote the borders of the 9/4 and 7/3 resonances.

(we recall that our integrations are not deterministic previews of future evolution, but just point out possible evolutionary paths).

The histogram of the distribution of the family with respect to the semi-major axis, reported in Fig. 13 (size limits of 40, 25, and 18), indicates that very probably, even within the size of completeness of the presently available sample (18 km), at least some 20 objects should have been injected into the resonance. A small anisotropy is probably recognizable looking at the right tail of the family beyond the resonance. However, the effect due to the resonance alone in depleting a part of the family is beyond any doubt. Therefore, since there are currently six members (including 1588) in the 9/4 resonance, we can estimate that about 50 to 75% of the original members have been eliminated up to now. From our numerical integrations (only one body in four is still in the family after 100 Myr) we can finally estimate that the age of the structure should be in the order of 100 Myr.

At this point two questions arise: should one consider 100 Myr to be the age of the whole Eos family? Where are the escaped resonant Eos family members now?

The answer to the first question is not certain. The apparent morphology of the Eos family in the space of proper elements challenges any attempt to model the event of its formation. In fact it is practically impossible to fit the present structure of the family by assuming an original isotropic field of fragment ejection velocities: the distribution of the family in the (a_P, e_P) plane is too spread in eccentricity. This suggests that either the original breakup was itself highly anisotropic or the present family is the final product of several multi-generational breakup events which involved the fragments originated in the primordial collision. In the last case 100 Myr could just be the age of one of these secondary events.

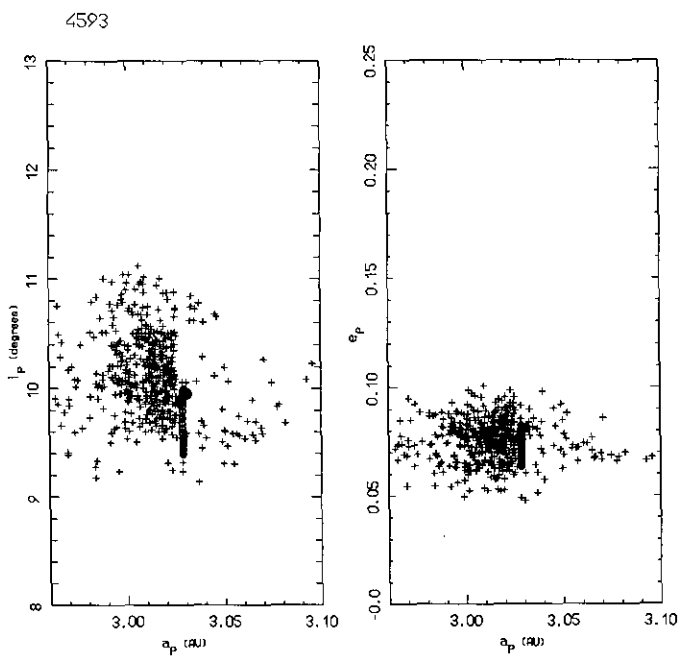

FIG. 12. The same as Fig. 9 but for the asteroid (4593) FV_1.

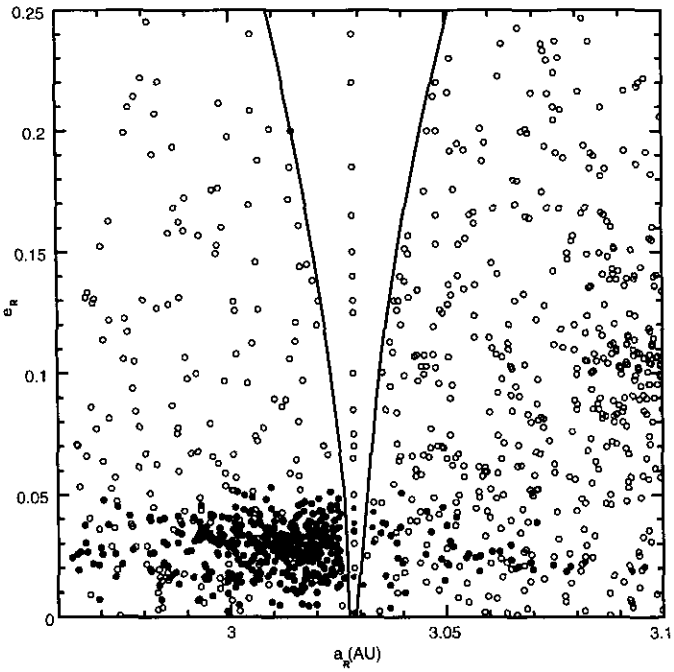

FIG. 14. The Eos family (solid circles) and the background objects (open circles) on the resonant proper plane (a_R, e_R), together with the limits of the 9/4 resonance. Moreover, 21 objects in the background are characterized by a resonant dynamics and therefore are plotted at a_R = 3.0285 AU. They are: 948, 992, 1465, 1630, 3120, 3341, 5212, 1881EB31, 1981EP2, 1981EJ8, 1985CD2, 1990QY, 1991AB1, 1991XS, 1290T1, 1066T2, 1356T2, 4087T2, 4105T2, 5366T2, 5077T3. We have to state that for some of them the corresponding dots cover each other.

The answer to the second question is even more delicate. We have carried on the numerical integrations of the four numbered asteroids described above, and, after 152 Myr, one of them, (4243) 1981 GF_1, reaches $e \simeq 0.4$, encounters Jupiter, and is ejected on a hyperbolic orbit. This shows that, at the end, a final depletion mechanism exists. However, we cannot state that the escaped resonant members of the Eos family have all been eliminated in this way; this seems incompatible with the fact that six resonant members are still in the family. Therefore, if our scenario of partial depletion is true, one should find, outside of the family, some more asteroids in the 9/4 resonance, on the way from the Eos family to Jupiter. With this conviction in mind, we have analyzed the whole asteroidal population located in the Eos zone, up to a proper eccentricity equal to 0.3; for each object, we have computed the resonant proper elements with respect to the 9/4 resonance, in order to select those which are inside the resonance from those which are outside. The result is illustrated in Fig. 14. We have found 21 bodies in this way, apart from those in the Eos family, which are presently connected to the 9/4 resonance. They are plotted at the center of the resonant region (a_R = 3.0285 AU), and the list of their names is provided in the figure legend. It is natural to conjecture that at least part of these bodies are escaped members of the Eos family. Luckily, the members of the Eos family have a peculiar taxonomic type; thus future physical observations of these bodies could (hopefully) definitely prove this conjecture.

6. QUASI ISOTROPIC FAMILIES

This section is devoted to three quasi-isotropic families: Dora, Gefion (Ceres), and Adeona. These families can be fitted by equivelocities curves so that we can provide an estimate of the fraction of original members which have been captured into the nearby mean motion resonances and, consequently, lost.

6.1. Dora

The Dora family is composed of 77 members (Zappalà *et al.* 1995) and represents a typical example of "cluster", i.e., a very deep and compact "stalactite" in the representation introduced by Zappalà *et al.* (1990). The distribution of the proper elements of the family indicates a quite strong relationship between eccentricity and semi-major axis. Following the procedure illustrated in section 3 it is possible to find in the (a, e) plane an EVC containing most of the family fragments. The best-fit EVC (obtained on the basis of a purely visual assessment) has been obtained for f = 70° and an isotropic velocity field of 100 m/sec. We have to notice that most of the objects which are located outside with respect to the above EVC are no longer family members when a more conservative value of the quasi random level (see Zappalà *et al.* 1990, 1994, 1995) is chosen. The distribution of the family, the corresponding best-fit EVC, and the boundaries of the 5/2 resonance are plotted in Fig. 15 with respect to the resonant proper semi-major axis and eccentricity. Referring to section 2, these correspond to the semi-mean a and e computed at $\sigma = 0$, $\tilde{\omega} - \tilde{\omega}_J = \pi$, and $\tilde{\omega} - \tilde{\omega}_S = 0$. At this configuration, all of the members of the family assume the minimal eccentricity during their quasi-periodic evolution.

From the figure, it appears that a nonnegligible fraction of the fragments ejected with a velocity smaller than about 100 m/sec may have reached the resonance. A more quantitative estimate can be obtained by looking at the histogram of Fig. 16. Here the filled part of the histogram refers to objects larger than 22 km, which is the size limit of the expected observational completeness for the Dora family. The other parts correspond to size limits of 15 and 10 km, and to the whole sample, respectively. A very qualitative look at Fig. 16 could indicate (on the basis of distribution symmetry arguments) that some five to six objects as large as 10–15 km could have been ejected into the 5/2 resonance. Such an estimate is in agreement with a simple

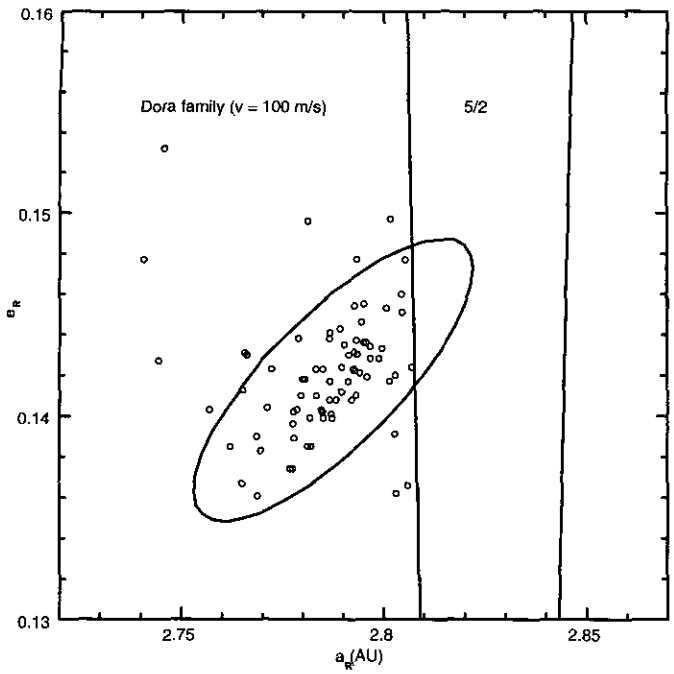

FIG. 15. The same as Fig. 6 but for the Dora family, together with the borders of the 5/2 resonance and the best-fit EVC (see text).

estimate based on looking at the relative fraction of the family volume associated with the resonance (see Fig. 15). However, this should be considered as a lower limit, since the family sample is incomplete at sizes smaller than 22 km. In addition, we have to take into account that smaller objects (i.e., ejected at higher velocity) can be contained in a EVC wider than that presented in Fig. 15, increasing, as a consequence, the number of fragments possibly injected into the 5/2 resonance. We can conclude that a conspicuous number of fragments have been injected into the 5/2 mean motion resonance with Jupiter and that a not negligible fraction of them can be as large as 10–15 km in size.

6.2. *Gefion (Ceres)*

The old Gefion family, identified by Zappalà *et al.* (1990, 1994), includes now, according to the most recent research by Zappalà *et al.* (1995), 84 nominal members, among which there are three large objects: 1 Ceres, 255 Oppavia, and 374 Burgundia (the last two having a diameter of about 50 km). However, the positions of 1, 255, and 374, denoted by solid circles in Fig. 17, are very peripheral with respect to the whole family; this suggests that possibly all of the new three entries are interlopers. This is confirmed by the fact that neither 1 nor 374 are found in the nominal list of members found by means of the WAM. Moreover, recent

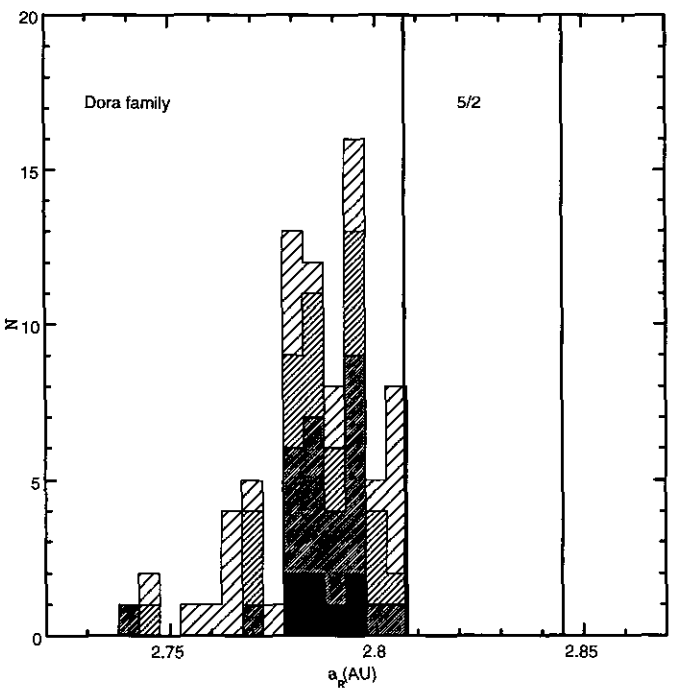

FIG. 16. The same as Fig. 7 but for the Dora family. The size limits are 22 (completeness limit), 15, 10 and 0 (whole sample) km. Vertical lines denote the borders of the 5/2 resonance computed for the average value of the resonant proper eccentricity of the Dora family.

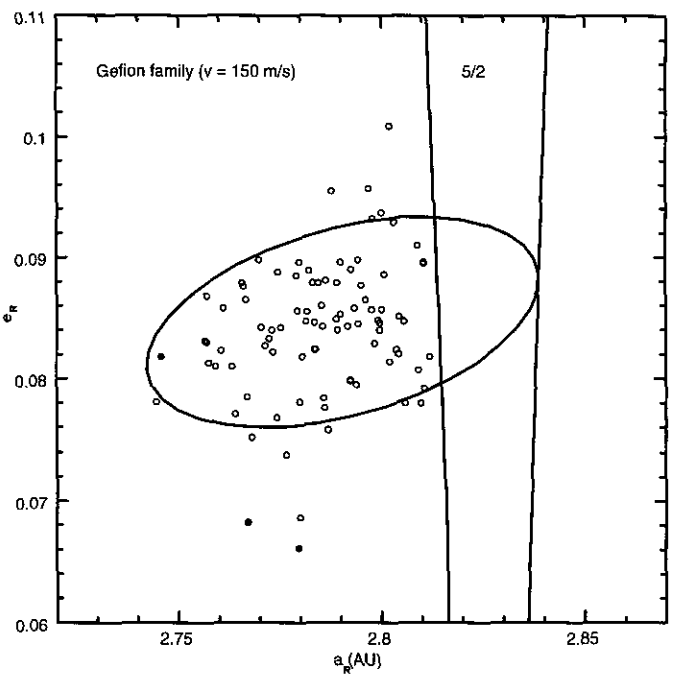

FIG. 17. The same as Fig. 6 but for the Gefion family together with the borders of the 5/2 resonance. Solid circles refer to the asteroids 1, 255, and 374, which could be considered as interlopers. The best-fit EVC is also indicated.

observations of several family members carried out by Binzel *et al.* (1994) show that the family is essentially composed of S-type asteroids. This is in conflict with the G-type classification of 1 Ceres, as well as with the very low albedo of 255 Oppavia (previously classified as an X-type). From this point of view, the situation of 374 Burgundia, which is an S-type object with a relatively high albedo (0.30), is not so clear.

For the above reasons, we prefer to continue to refer to this family as the Gefion family. Nevertheless, the figures of the present paper include all of the nominal members, including the three large ones. On the other hand, we have to point out that if they are proved to belong genetically to this family, any assumption of isotropy will have to be ruled out. For the moment, we prefer to assume an isotropic velocity field centered in the barycentre of the family computed with the exclusion of the three largest objects. However, the importance of the 5/2 resonance would probably not change even in the case of some anisotropic configuration.

The EVC containing most of the fragments has been obtained for $f = 85°$ and for a velocity of 150 m/sec, as reported in Fig. 17. The histogram of the distribution with respect to a_R is shown in Fig. 18. Here, the size limits corresponding to the differently shaded parts of the histogram are 25, 17 (the completeness diameter), and 10 km and the whole sample, respectively.

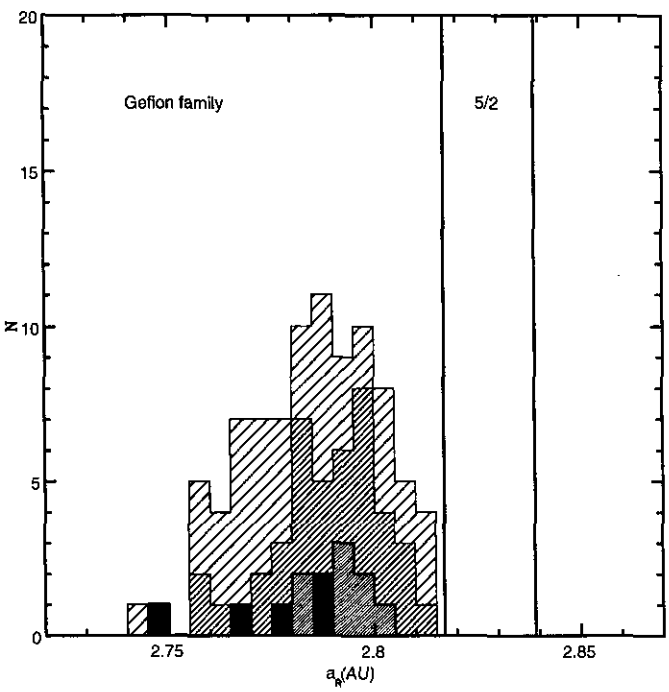

FIG. 18. The same as Fig. 7 but for the Gefion family. Size limits are 25, 17 (completeness limit), 10, and 0 (whole sample) km. Vertical lines denote the borders of the 5/2 resonance.

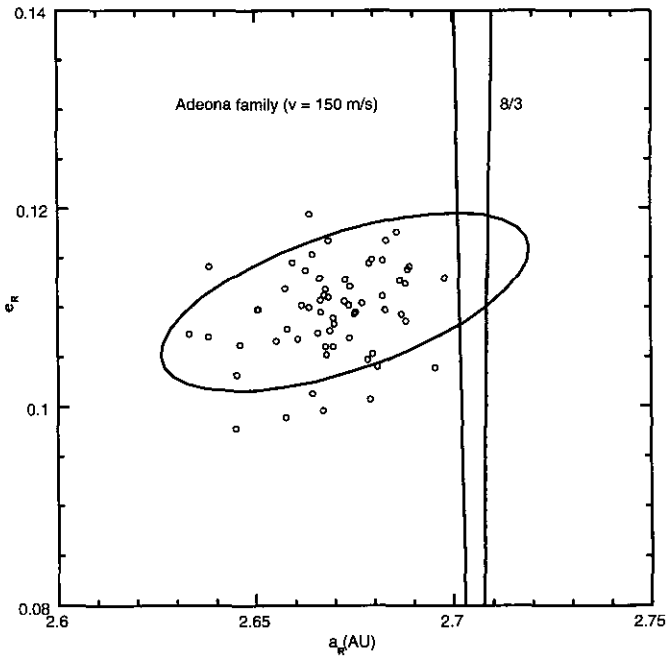

FIG. 19. The same as Fig. 6 but for the Adeona family, together with the 8/3 resonance and the best-fit EVC.

Figures 17 and 18 seem to indicate that the high a border of the family is cut by the 5/2 mean motion resonance. Objects as large as about 15 km could have been affected by this process. All of the considerations concerning the (presumably larger) real consistence of the family extrapolated to smaller sizes (i.e., to higher velocities) which have been pointed out in the case of the Dora family can be repeated also in the case of the Gefion family.

In Figs. 17 and 18 the resonant proper a_R and e_R have been computed at $\sigma = 0$, $\tilde{\omega} - \tilde{\omega}_J = \pi$, and $\tilde{\omega} - \tilde{\omega}_S = 0$ (see section 2). We have remarked, looking at numerical integrations, that the secondary resonance with argument $\tilde{\omega} - 2\tilde{\omega}_S + \tilde{\omega}_J$ has some influence, modulating the distance asteroid–resonance border over a 1-Myr timescale. Taking into account this phenomenon, however, would not change in a significant way the results reported in the above figures.

6.3. *Adeona*

Adeona is another case for which an isotropic configuration can be accepted. This family is formed by 63 members (Zappalà *et al.* 1995). The best-fit EVC has been obtained for $f = 80°$ and $V = 150$ m/sec. Figure 19 shows the family, the EVC, and the 8/3 mean motion resonance. The semi-major axis distribution for different size ranges is shown in Fig. 20. Here, the size limits are 100, 17, and 10 km, respectively. The completeness size is 17 km. On the basis

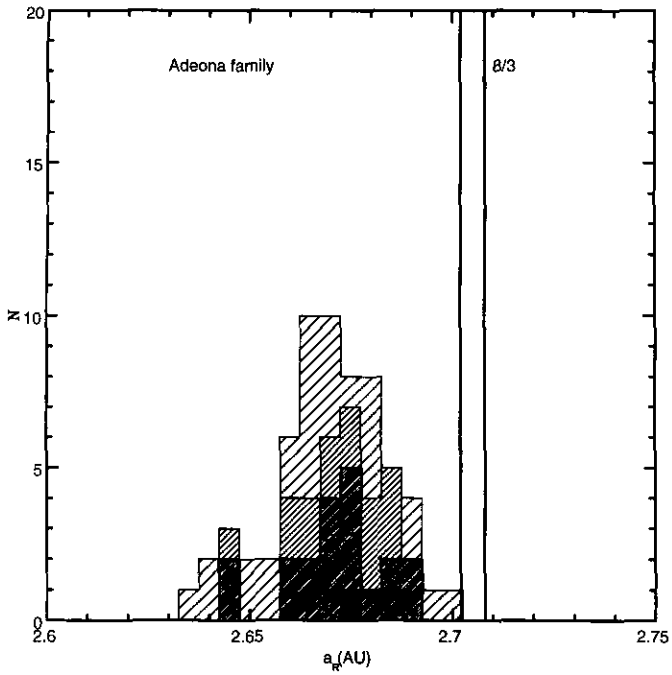

FIG. 20. The same as Fig. 7 but for the Adeona family. Size limits are 100, 17 (completeness size), 10, and 0 (whole sample) km. Vertical lines denote the borders of the 8/3 resonance, computed for the average value of the resonant proper eccentricity of the family.

of the data shown in Fig. 20, it is suggested that the resonance should have affected only marginally the original distribution, while the EVC might indicate some injection inside the resonance or even beyond its other side. This last possibility has been checked without any positive result, by means of a visual search for objects located close to the inner resonance edge and in the same interval of e_P and i_P shown by the family. However, due to the incompleteness of the currently available sample, we cannot exclude that the situation could change when new data is available.

In Figs. 19 and 20 the resonant proper a_R and e_R are computed at $\sigma = 0$, $\tilde{\omega} - \tilde{\omega}_J = \pi$, and $\tilde{\omega} - \tilde{\omega}_S = 0$, which correspond to the minimal eccentricity of all of the family members.

7. NON-ISOTROPIC FAMILIES

This section is devoted to the nonisotropic families of Eunomia, Maria, Nysa, and Hygiea. For these families it is more difficult to estimate quantitatively the fraction of members injected into the Kirkwood gaps. However, the analysis of their distribution with respect to mean motion resonances can suggest some conjectures on the origin of particular classes of near Earth objects of particular taxonomic types.

7.1. *Eunomia*

Eunomia is one of the most populous families recognized in the belt. According to Zappalà *et al.* (1995), it contains 439 members. The configuration in the (a_P, e_P) plane does not strictly suggest an original isotropic ejection of the fragments, although this possibility cannot be ruled out. In addition to the complexity of its distribution in the (a_P, e_P) plane, we have to take into account the fact that this family seems to be composed of both S-type objects and C-type ones. This seems to rule out a single cosmochemically plausible parent body for the whole family. One possibility is that the family is the result of a superimposition of two distinct events coming from two different parent bodies due only to chance (see also Cellino and Zappalà 1993). Statistics alone are not able to separate the events and must be supported by observational campaigns aimed at determining the taxonomic types of a large number of members. Figure 22, which shows the a histogram for different size ranges (20, 15, and 10 km, with the latter being the completeness size), gives some indication of a complex distribution, with two or three separate peaks. Note that these peaks are recognizable in most of the chosen size ranges.

Figure 21 shows the distribution of the family on the proper resonant plane (a_R, e_R), together with the borders of the 3/1 and 8/3 resonances. While the 3/1 resonance appears to be far from the border of the Eunomia family (but we should bear in mind that we cannot say anything about the dispersion of fragments much smaller than the observed ones), this family crosses the 8/3 resonance, with some indication that part of the tail of the fragment distribution at larger a_R may have been affected by this resonance.

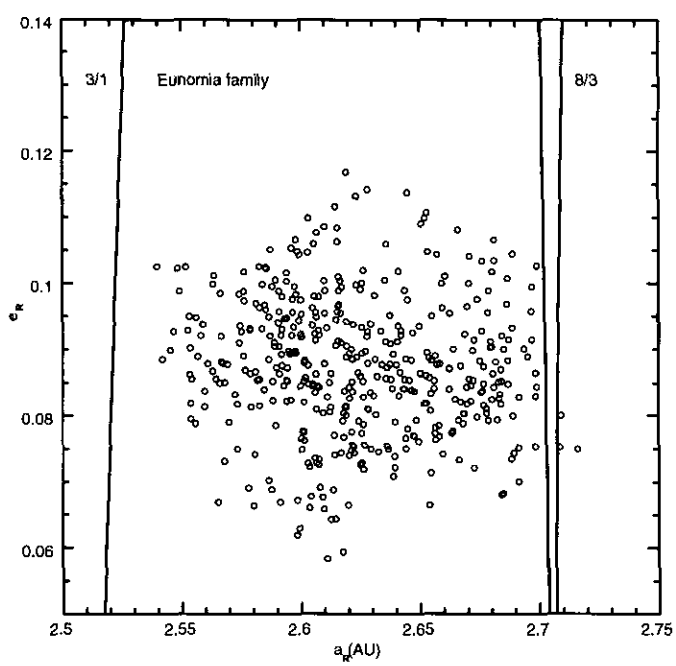

FIG. 21. The same as Fig. 6 but for the Eunomia family together with the borders of the 3/1 and 8/3 resonances.

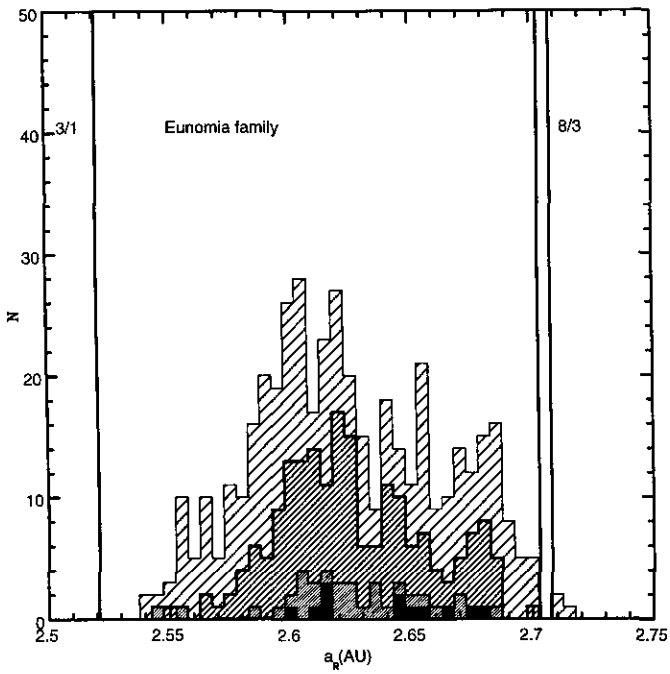

FIG. 22. The same as Fig. 7 but for the Eunomia family. Size limits are 20, 15, 10 (completeness size), and 0 (whole sample) km. The vertical lines denote the borders of the 3/1 and 8/3 resonances.

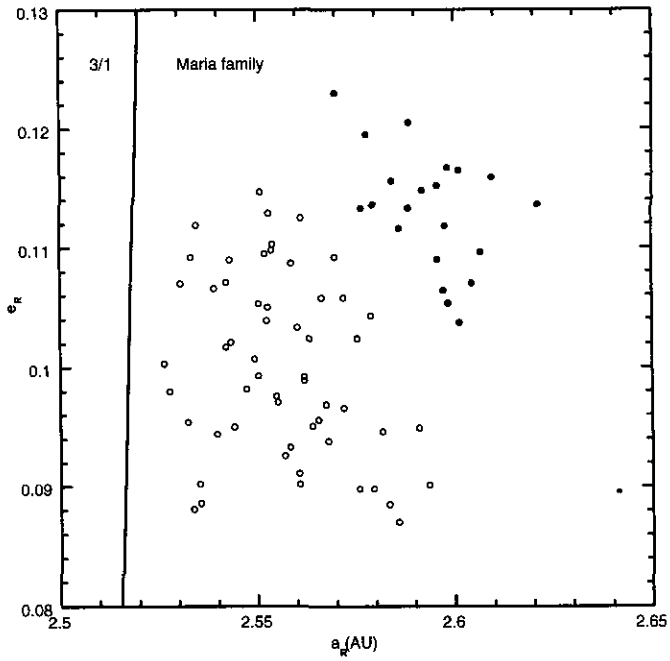

FIG. 23. The same as Fig. 6 but for the Maria family together with the separatrix of the 3/1 resonance. Solid circles refer to a subgrouping which leaves the main group 10 m/sec below the nominal QRL.

In Figs. 21 and 22 the resonant proper a_R and e_R are computed at $\sigma = 0$, $\tilde{\omega} - \tilde{\omega}_J = \pi$, and $\tilde{\omega} - \tilde{\omega}_S = 0$.

7.2. *Maria*

This high inclination family was already recognized by Hirayama in his pioneering work at the beginning of the present century. However, the structure appears quite complex, as can be seen in Fig. 23, where the right border of the 3/1 mean motion resonance is plotted together with the (a_R, e_R) distribution of the family members. According to Zappalà *et al.* (1995), changing by 10–20 m/sec the quasi random level (QRL, the criterion used for defining the nominal membership above a given statistical reliability), the morphology of the family can change drastically. In particular, one subgrouping (indicated by solid circles in the figure) leaves the main group 10 m/sec below the nominal QRL. It follows that any assumption about an isotropic configuration is currently very premature and difficult to support. We cannot disregard the possibility that the whole family reflects a complex collisional history involving two (or more) subsequent events. The a histogram for different size ranges is shown in Fig. 24, where the size limits are 20 and 10 km (with the latter being the completeness size). Although the 3/1 resonance appears quite far from the edge of the present family, the concentration of large objects toward its border could indicate that an original isotropic structure may have been severely affected by the

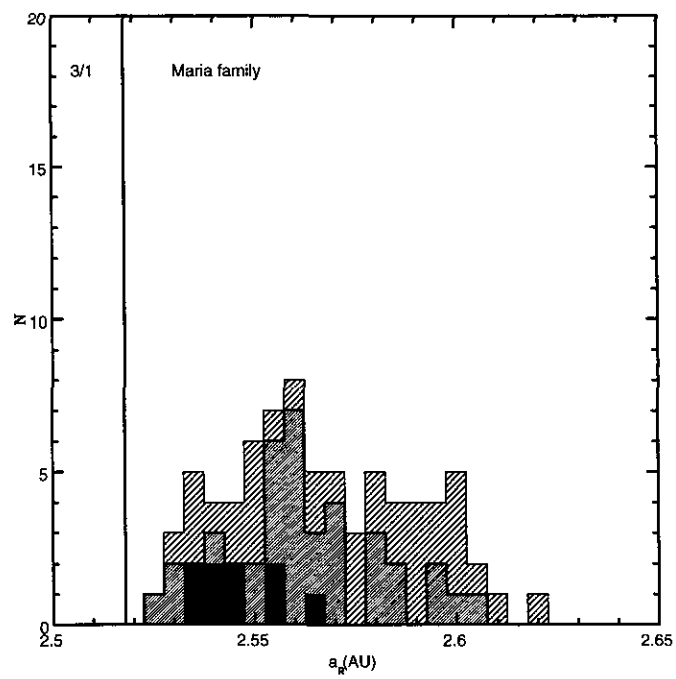

FIG. 24. The same as Fig. 7 but for the Maria family. Size limits are 20, 10 (completeness limit), and 0 (whole sample) km. The vertical line denotes the outer border of the 3/1 resonance, computed for the average value of the resonant proper eccentricity of the family.

resonance. In particular, even quite large objects ($D \geq 20$ km) could have been involved in this process. If we take into account that the Maria family is probably the only one composed of S-type objects which can have injected large asteroids into the inner planetary region, it follows that a further study is very important mainly in view of the problem of the origin of the "giant" Apollo-Amor objects 1036 Ganymede and 433 Eros, both classified as S-type. We have to remark that only a big catastrophic event can produce fragments as big as these two asteroids, and it seems reasonable to predict that such an event should produce a well-observable family.

In Figs. 23 and 24 the resonant proper a_R and e_R are computed at $\sigma = \pi/2$, $\tilde{\omega} - \tilde{\omega}_J = \pi$, and $\tilde{\omega} - \tilde{\omega}_S = \pi$.

7.3. Nysa

According to the nomenclature proposed by Farinella *et al.* (1992), the one associated with Nysa is a typical *clan*, since it is far from being a sharp and well-defined grouping. Two major clusters (the Nysa and Polana families) join together at a level only 10 m/sec higher than the QRL of 120 m/s (Zappalà *et al.*, 1995). In the present analysis we consider the two families together as they are found at the distance level of 130 m/s, but we have to point out that the clan is a very complex structure possibly reflecting a complex, multi-generational impact history starting from a primordial, very old, original breakup of a differentiated parent body. The physical properties and a possible evolutionary scenario of the Nysa clan will be discussed in a forthcoming paper, in preparation; here, we limit the discussion only to any possible relation with the 3/1 mean motion resonance with Jupiter. The complexity of the clan is evident in Fig. 25, which shows the (a_R, e_R) distribution, together with the 3/1 resonance. Figure 26 gives the a histogram for size limits of 25, 15, 10, and 5 km, (with 10 km being the completeness size), where a bimodality seems fairly evident. For this family, we did not use the albedo of the IRAS-observed members in order to compute the sizes of the objects lacking an albedo estimate. This is due to the occurrence of a large albedo nonhomogeneity, related to the simultaneous presence of Nysa itself, a bright E-type asteroid, and several low albedo F objects. For this reason, we assumed the fixed value of 0.05 for the albedo of the objects not observed by IRAS. Such a value is typical of F-type objects.

We have to notice that the larger bodies are located preferentially in the right part of Fig. 26. At first glance, it seems that the clan has not been affected by the resonance; however, this conclusion could be premature. In fact, a number of F-type objects are present in this zone of the (a, e, i) space which, even though they are not members of the clan at the nominal QRL (according to Zappalà *et al.* 1995), join the family at levels higher than the QRL. Moreover, some F-type objects do nominally belong to either of the two subgroupings of Nysa and Polana. Another important fact to be kept in mind is that the F-type

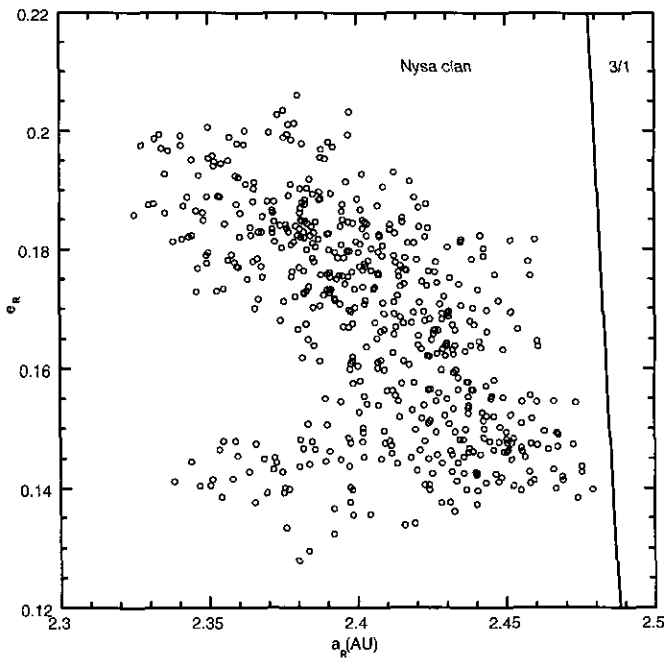

FIG. 25. The same as Fig. 6 but for the Nysa clan together with the separatrix of the 3/1 resonance.

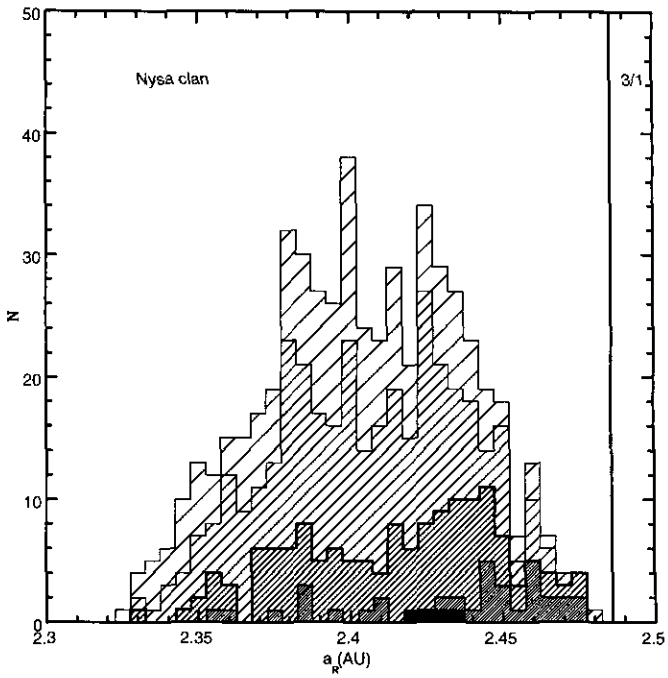

FIG. 26. The same as Fig. 7 but for the Nysa clan. Size limits are 25, 15, 10 (completeness size), 5, and 0 (whole sample) km. The vertical line denotes the inner border of the 3/1 resonance.

object 3200 Phaeton is a well-known near Earth asteroid, while 4015 Wilson Harrington, an Apollo object that has been recently found to show a cometary activity, was also formerly classified as a CF asteroid (Tholen 1984). Taking into account the efficiency of the 3/1 resonance in injecting objects into the inner planetary region (Morbidelli and Moons 1995), and considering that F-type asteroids are rare in the inner regions of the belt, (apart from those apparently associated with the Nysa clan), the idea that a nonnegligible number of F fragments originating from the Nysa clan entered the resonance cannot be completely ruled out. A possible comprehensive scenario will be presented in a further paper in preparation.

In Figs. 25 and 26 the resonant proper a_R and e_R are computed at $\sigma = \pi/2$, $\tilde{\omega} - \tilde{\omega}_J = \pi$, and $\tilde{\omega} - \tilde{\omega}_S = \pi$.

7.4. *Hygiea*

The recent possibility of analyzing large data sets of asteroid proper elements, including a very high number of faint objects, has led to the identification of families mainly composed of swarms of faint members (Zappalà *et al.* 1994, 1995). Among these groupings, particularly important is the one associated with the very large asteroid 10 Hygiea. With an IRAS-derived diameter of 407 km, 10 Hygiea is the largest C-type object in the asteroid belt. According to Zappalà *et al.* (1995), 10 Hygiea has an associated family formed by 103 members, including a large fraction of objects less than 10 km in size. A few sizable objects with D around 80 km (100, 353, 538) are probable interlopers, as suggested also by the high albedo value in the case of 100 Hekate.

Due to the large size of 10 Hygiea, we are dealing here with a family which should be considered as the outcome of a very energetic *cratering* event, that is, an impact which did not disrupt totally or partially the parent body, but created a large crater, whose ejecta formed the observable family. Therefore, any representation of EVC curves is not appropriate in this case, since any assumption of isotropic ejection of the fragments can be ruled out for such kinds of impact. In this respect, this family is similar to the other, well-known, case of Vesta.

However, Fig. 27 shows that the proximity of the 2/1 resonance could have influenced the present morphology of this family. The resonant proper semi-major axis and eccentricity adopted here are similar to the case of Themis described above. In particular, they are the values that the mean a and e assume for $\sigma = 0$, $\tilde{\omega} - \tilde{\omega}_J = 0$, and $\tilde{\omega} - \tilde{\omega}_S = \pi$. The figure shows that the edge of the resonance seems to cut the outer border of the family, going toward larger values of a. This inference is confirmed by the appearance of the semi-major axis distribution for different size ranges, shown in Fig. 28. The different shadings correspond to values of 25 km, 10 km and the whole sample,

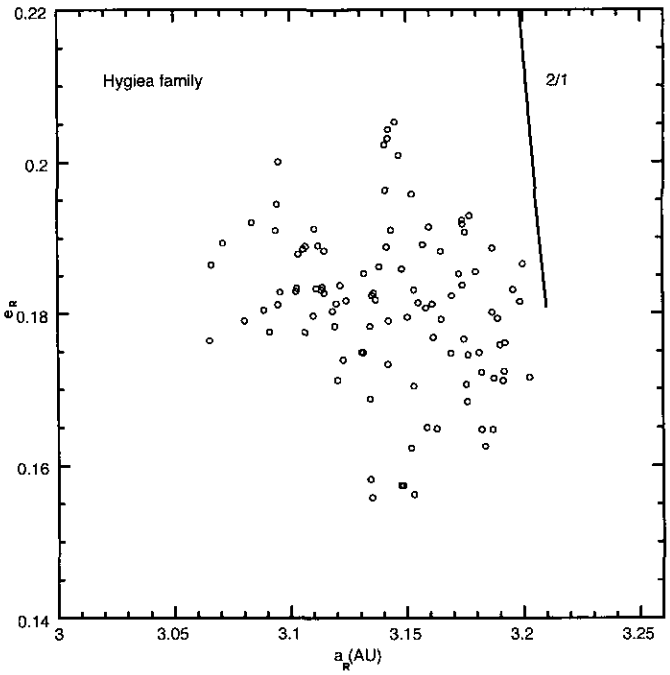

FIG. 27. The same as Fig. 6 but for the Hygiea family, together with the separatrix of the 2/1 resonance. We recall that the leftmost separatrix of the 2/1 resonance is defined only for $e_R > 0.18$ (see also Fig. 6).

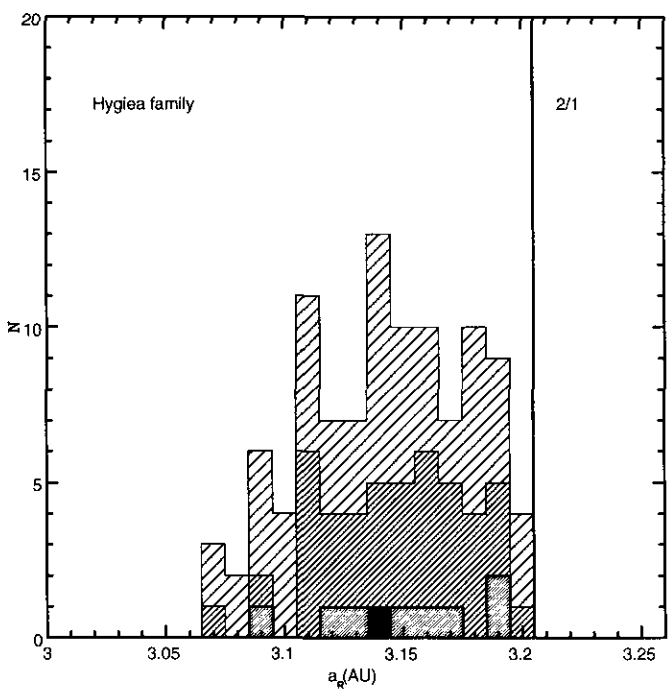

FIG. 28. The same as Fig. 7 but for the Hygiea family. Size limits are 25 (completeness size), 10, and 0 (whole sample) km. Hygiea itself is represented by the mean of the filled bin. The vertical line denotes the inner border of the 2/1 resonance.

respectively. Hygiea itself is represented by means of the filled bin. The completeness diameter is 25 km for this family. The histogram suggests that a significant fraction of the original tail of the distribution toward larger heliocentric distances may have been depleted by the resonance. This fact strengthens the conclusions about the importance of the 2/1 mean motion resonance with Jupiter as an efficient asteroid sweeper already obtained by the analysis of the Themis family.

8. CONCLUSIONS

The present work constitutes a necessary prerequisite for the development of a detailed physical analysis of the asteroid families. Its aim is to evaluate the effect that mean motion resonances can have on the structure of nearby families. In particular, we have checked whether some original family members could have been captured into a resonance and subsequently eliminated.

To achieve this goal, we have developed in section 2 a theory on the secular motion of objects close to mean motion resonances, which leads to the definition of new *resonant proper elements*. These in turn allow us to compare properly the distribution of the family members with the extension of the resonant zones. This theory, which is based on the concept of adiabatic capture into mean motion resonances due to secular variations of orbital elements, unfortunately does not work for the Koronis family. Therefore, the Koronis family has not been analyzed in this paper.

Furthermore, many small families close to mean motion resonances, identified by Zappalà *et al.* (1995), have not been analyzed here, since any conclusion would be very uncertain due to the very small amount of known family members. We plan to analyze these families in the future, as soon as the discovery of new asteroids extends the number of the recognized family members.

In this paper, we have concentrated our analysis on the big families of Themis, Eos, Gefion, Dora, Adeona, Eunomia, Maria, Nysa, and Hygiea. The main results that we have obtained are the following:

- The Themis family is sharply delimited by the border of the 2/1 mean motion resonance. It is unlikely to believe that this striking feature is due to chance. So we conjecture that many members of the Themis family have been injected into the 2/1 mean motion resonance and depleted by resonant dynamics. It is true that the 2/1 Kirkwood gap is not completely understood, up to now, by celestial mechanicians. However, the region of the 2/1 resonance which could have been filled by Themis members has been found to be unstable in the recent work by Henrard *et al.* (1995). The asteroid 3789 Zhongguo which is presently inside the 2/1 mean motion resonance and seems to be in an island of stability, at least over long timescales, is on the ideal prolongation of the Themis family into the 2/1 resonance and therefore could be a family member. Similar conclusions on the depleting role of the 2/1 resonance are also suggested by the family of Hygiea, which can be described as the outcome of a big cratering event.
- The density of the members of the Eos family drops at the border of the 9/4 resonance. However, a few members of the family are currently in the resonance. Our numerical integrations over 100 Myr show that all of these objects are chaotic and will abandon the Eos family due to relevant changes in their eccentricity and inclination. Eventually, they can become Jupiter-crossers and be ejected into hyperbolic orbits. Therefore, we suggest that the members of the Eos family which are currently in the 9/4 resonance are possibly young, probably the product of a secondary event. Moreover, we guess that the asteroids which are currently in the 9/4 resonance, but which have not been recognized to belong to the Eos family, can be Eos members which already escaped the family region.
- The families of Gefion and Dora could have injected a significant fraction of their members into the 5/2 mean motion resonance; Adeona is marginally affected by the 8/3 resonance. Their good fit with isotropic breakup models allow us to quantify roughly the amount of fragments injected into the nearby resonances and the plausible maximum sizes of these objects.
- The structures of the families of Eunomia, Nysa, and Maria do not provide definite indications of the role played by nearby mean motion resonances. This is mainly due to the complex structure of these families, which can hardly be fitted by single isotropic models. Eunomia extends through the 8/3 resonance, and just a very narrow gap is visible. Nysa and Maria are located quite close to the 3/1 resonance, but it is not evident that the limits of the families coincide with the resonance borders. Nevertheless, among all of the families, Maria is the one that could have injected the biggest bodies into a mean motion resonance. It is then tempting to guess that the most massive near Earth asteroids could come from the Maria family through the 3/1 resonance; this conjecture can be confirmed or rejected only on the basis of the physical properties of both Maria members and giant NEAs. On the other hand, the F-type objects associated with the Nysa grouping could have some relationship with the few F-type NEAs. We recall that F asteroids are extremely rare in the inner belt, with the Nysa clan location being the only exception.

In light of these results, we can say that that the present work does not concern only the structure of asteroid families, but also the problem of the origin of near Earth asteroids and meteorites and, particularly, of those having a relatively large size. Indeed, in the case of the families studied in this paper, we have (i) the evidence that a breakup occurred and (ii) a very strong indication that a

relevant fraction of the original members, even at appreciable sizes, have been lost into the resonant Kirkwood gaps, from which we expect an Earth-crossing orbit with large eccentricity. In particular, this is very important for what concerns the origin of the few relatively large NEAs: objects like 433 Eros cannot be considered to belong to the low-size, high-speed tail of the fragment distribution from any generic event. NEAs beyond 20 km in size should have been produced in energetic events, and the most obvious candidates are the events which produced the most important families recognizable today. Taking into account that an inverse size ejection velocity is suggested by laboratory experiments and physical modeling (and is also confirmed by the families identified in the main belt), it is obvious that objects like 433 Eros should have been created *close* to some important resonance. Thus, the most plausible parent families are those analyzed in the present paper.

REFERENCES

BENDJOYA, PH. 1993. A classification of 6479 asteroids into families by means of the wavelet clustering method. *Astron. Astrophys. Suppl. Ser.* **102,** 25–55.

BENDJOYA, PH., E. SLEZAK, AND C. FROESCHLÉ 1991. The wavelet transform: A new tool for asteroid family determination. *Astron. Astrophys.* **251,** 312–330.

BENDJOYA, PH., A. CELLINO, C. FROESCHLÉ, AND V. ZAPPALÀ 1993. Asteroid dynamical families: A reliability test for two identification methods. *Astron. Astrophys.* **272,** 651–670.

BENZ, W., AND E. ASPHAUG 1994. Impact simulations with fracture. I. Methods and tests. *Icarus* **107,** 98–116.

BENZ, W., E. ASPHAUG, AND E. V. RYAN 1994. Numerical simulations of catastrophic disruption: Recent results. *Planet. Space. Sci.* **42,** 1053–1066.

BINZEL, R. P., AND S. XU 1993. Chips off of asteroid 4 Vesta: Evidence for the parent body of basaltic achondrite meteorites. *Science* **260,** 186–190.

BINZEL, R. P., S. J. BUS AND S. XU 1994. Physical studies of small asteroid families. *Bull Am. Astron. Soc.* **26,** 1178.

BOTTKE, W. F., M. C. NOLAN, R. GREENBERG, AND R. A. KOLVOORD 1994. Velocity distribution among colliding asteroids. *Icarus* **107,** 255–268.

BROUWER, D. 1951. Secular variations of the orbital elements of minor planets. *Astron. J.* **56,** 9–32.

CELLINO, A. AND V. ZAPPALÀ 1993. Asteroid clans: Super families or multiple events? *Celest. Mech. Dynam. Astron.* **57,** 37–47.

DERMOTT, S. AND C. MURRAY 1983. Nature of the Kirkwood gaps in the asteroid belt. *Nature* **301,** 201–205.

FARINELLA, P., R. GONCZI, CH. FROESCHLÉ, AND C. FROESCHLÉ 1993. The injection of asteroid fragments into resonances. *Icarus* **101,** 174–187.

FARINELLA, P., AND D. R. DAVIS 1992. Collision rates and impact velocities in the main asteroid belt. *Icarus* **97,** 111–123.

FARINELLA, P., D. R. DAVIS, A. CELLINO, AND V. ZAPPALÀ 1992. From clusters to families: A proposal for a new nomenclature. In *Asteroids Comets Meteors 1991* (A. W. Harris and E. Bowell, Eds.), pp. 165–166. Lunar Planet Inst., Houston.

FUJIWARA, A., P. CERRONI D. R. DAVIS, E. RYAN, M. DI MARTINO, K. HOLSAPPLE AND K. HOUSEN 1989. Experiments and scaling laws on catastrophic collisions. In *Asteroids II* (R. P. Binzel, T. Gehrels, and M. S. Matthews, Eds.), pp. 240–265, Univ. of Arizona Press, Tucson.

GREENBERG, R., AND M. C. NOLAN 1989. Delivery of asteroids and meteorites to the inner Solar System. In *Asteroids II* (R. P. Binzel, T. Gehrels, and M. S. Matthews, Eds.), pp. 778–804. Univ. Arizona Press, Tucson.

HENRARD, J., AND A. LEMAITRE 1983a. A second fundamental model for resonance. *Celest. Mech. Dynam. Astron.* **30,** 197–218.

HENRARD, J., AND A. LEMAITRE 1983b. A mechanism of formation for the Kirkwood gaps. *Icarus* **55,** 482–494.

HENRARD, J., N. WATANABE AND M. MOONS 1995. A bridge between secondary and secular resonances inside the Hecuba gap. *Icarus* **115,** 336–346.

KNEŽEVIĆ, Z. AND A. MILANI 1994. Asteroid proper elements: The big picture. In *Asteroids, Comets, Meteors 1993* (A. Milani, M. Di Martino, and A. Cellino, Eds.), 143–158. Kluwer Academic, Dordrecht.

LEMAITRE, A. 1984. High-order resonances in the restricted three-body problem. *Celest. Mech. Dynam. Astron.* **32,** 109–126.

LINDBLAD, B. A. 1992. A computer search for asteroid families. In *Asteroids Comets Meteors 1991* (A. W. Harris, and E. Bowell, Eds.), pp. 363–366. Lunar Planet Inst., Houston.

LINDBLAD, B. A. 1994. A study of asteroid dynamical families. In *75 Years of the Hirayama Asteroid Families: The Role of Collisions in the Solar System History* Astronomical Society of the Pacific Conference Series, (Y. Kozai, R. P. Binzel, and T. Hirayama, Eds.), Vol **63,** pp. 63–75. Astronomical Society of the Pacific, San Francisco.

MALHOTRA, R. 1994. Nonlinear resonances in the solar system. *Physica D* **77,** 289–304.

MARZARI, F., D. R. DAVIS, AND V. VANZANI 1995. Collisional evolution of asteroid families. *Icarus* **113,** 168–187.

MELOSH, H. J., E. V. RYAN, AND E. ASPHAUG 1992. Dynamic fragmentation in impacts: Hydrocode simulation of laboratory impacts. *J. Geophys. Res.* **97/E9,** 14735–14759.

MILANI, A., AND Z. KNEŽEVIĆ 1990. Secular perturbation theory and computation of asteroid proper elements. *Celest. Mech. Dynam. Astron.* **49,** 347–411.

MILANI, A., AND Z. KNEŽEVIĆ 1992. Asteroid proper elements and secular resonances. *Icarus* **98,** 211–232.

MILANI, A., AND Z. KNEŽEVIĆ 1994. Asteroid proper elements and the dynamical structure of the asteroid main belt. *Icarus* **107,** 219–254.

MILANI, A., AND P. FARINELLA 1994. The age of the Veritas asteroid family deduced by chaotic chronology. *Nature* **370,** 40–42.

MILANI, A., AND P. FARINELLA 1995. An asteroid on the brink. *Icarus* **115,** 209–242.

MOONS, M. 1994. Extended Schubart Averaging. *Celest. Mech. Dynam. Astron.* **60,** 173–186.

MOONS, M., AND A. MORBIDELLI 1995. Secular resonances inside mean motion commensurabilities: The 4/1, 3/1, 5/2 and 7/3 cases. *Icarus* **114,** 36–50.

MORBIDELLI, A., AND M. MOONS 1993. Secular resonances inside mean motion commensurabilities: The 2/1 and 3/2 cases. *Icarus* **102,** 316–332.

MORBIDELLI, A., AND M. MOONS 1995. Numerical evidences on the chaotic nature of the 3/1 commensurability. *Icarus* **115,** 60–65.

NOBILI, A., A. MILANI AND M. CARPINO 1989. Fundamental frequencies and small divisors in the orbits of the outer planets. *Astron. Astrophys.* **210,** 313–336.

PAOLICCHI, P., A. CELLINO, P. FARINELLA AND V. ZAPPALÀ 1989. A semiempirical model of catastrophic breakup processes. *Icarus,* **77,** 187–212.

PAOLICCHI, P., A. VERLICCHI AND A. CELLINO 1993. Catastrophic fragmentation and formation of families: Preliminary results from a new numerical model. *Celest. Mech. Dynam. Astron.* **57,** 49–56.

PAOLICCHI, P., A. VERLICCHI, AND A. CELLINO 1994. An improved semi-empirical model of catastrophic impact processes. I. Theory and laboratory experiments. *Icarus* submitted.

SCHUBART, J. 1978. New results on the commensurability cases of the problem Sun-Jupiter-asteroid. In *Dynamics of Planets and Satellites and Theories of Their Motion* (V. Szebehely, Ed.), pp. 137–143. D. Reidel, Dordrecht.

STOER, J., AND R. BULIRSCH 1980. *Introduction to Numerical Analysis*. Springer–Verlag, New York.

TEDESCO, E. F., G. J. VEEDER, J. W. FOWLER, J. R. CHILLEMI 1992. The IRAS minor planet survey. Phillips Laboratory, Hanscom Air Force Base.

THOLEN, D. J. 1984. *Asteroid Taxonomy from Cluster Analysis of Photometry*. Ph.D. Thesis, Univ. of Arizona, Tucson.

VERLICCHI, A., A. LA SPINA, P. PAOLICCHI, AND A. CELLINO 1994. The interpretation of laboratory experiments in the framework of an improved semi-empirical model. *Planet. Space Sci.* **42,** 1031–1043.

WISDOM, J. 1983. Chaotic behavior and the origin of the 3/1 Kirkwood gap. *Icarus* **56,** 51–74.

WISDOM, J. 1985. A perturbative treatment of the motion near the 3/1 commensurability. *Icarus* **63,** 272–289.

WISDOM, J. 1986. *Chaotic Dynamics in the Solar System*. Text of the Urey Lecture, November 1986, Paris, France.

YOSHIKAWA, M. 1990. Motions of asteroids at the Kirkwood gaps. I. On the 3:1 resonance with Jupiter. *Icarus* **87,** 78–102.

YOSHIKAWA, M. 1991. Motions of asteroids at the Kirkwood gaps. II. On the 5:2, 7:3 and 2:1 resonances with Jupiter. *Icarus* **92,** 94–117.

ZAPPALÀ, V., AND A. CELLINO 1994. Asteroid families. In *Asteroids, Comets, Meteors 1993* (A. Milani, M. Di Martino, and A. Cellino, Eds.), pp. 395–414, Kluwer Academic, Dordrecht.

ZAPPALÀ, V., AND A. CELLINO 1995. Main belt asteroids. Present and future inventory. Astronomical Society of the Pacific Conference Series, in press.

ZAPPALÀ, V., A. CELLINO, P. FARINELLA, AND Z. KNEŽEVIĆ 1990. Asteroid families. I. Identification by hierarchical clustering and reliability assessment. *Astron. J.* **100,** 2030–2046.

ZAPPALÀ, V., A. CELLINO, P. FARINELLA, AND A. MILANI 1994. Asteroid families. II. Extension to unnumbered multiopposition asteroids. *Astron. J.* **107,** 772–801.

ZAPPALÀ, V., PH. BENDJOYA, A. CELLINO, P. FARINELLA, AND C. FROESCHLÉ 1995. Asteroid families: Search in a 12,487 asteroid sample with two different clustering techniques. *Icarus* **116,** 291–314.